Chapter 15
Stochastic Löwner Evolution and the Scaling Limit of Critical Models

Bernard Nienhuis and Wouter Kager

15.1 Introduction

Great progress in the understanding of conformally invariant scaling limits of stochastic models, has been given by the Stochastic Löwner Evolutions (SLE). This approach has been pioneered by Schramm [46] and by Lawler, Schramm and Werner [31]. It describes a one-parameter family of conformally invariant measures of curves in the plane or a two-dimensional domain. This family is commonly referred to as SLE_κ, where κ parametrizes the family. It has been shown to be the scaling limit of many well-known and less well-known statistical lattice models. These models are typically members of the families of critical and tricritical [40] q-state Potts models [61] and of O(n) models [17], or believed to be in the corresponding universality class.

SLE describes the scaling limit of various open, non-crossing, stochastic paths on the lattice, which are, at least on one side, attached to the boundary. Therefore its application to polygons is restricted in various ways. In the first place it describes only the scaling limit. In many studies of lattice polygons, of course, the scaling limit is considered the most interesting aspect. The restriction to open paths attached to the boundary is more severe. This restriction has been lifted to some extent by recursively considering domains bounded by closed paths resulting from a previous SLE process. This approach applies only to paths that have a tendency to touch themselves (without, of course crossing), and this generalization is not the subject of this chapter. In most cases the paths under consideration by their nature occur in extensive numbers. However, one may concentrate on one of them, and treat the

Bernard Nienhuis
Institute for Theoretical Physics, University of Amsterdam, 1018 XE Amsterdam, The Netherlands, e-mail: b.nienhuis@uva.nl

Wouter Kager
VU University Amsterdam, Department of Mathematics, De Boelelaan, 1081 HV Amsterdam, The Netherlands, e-mail: wkager@few.vu.nl

interaction with the others only as an ingredient that defines the stochastic measure of the path under consideration. This, in fact is precisely what SLE does.

So far the essential progress made by the SLE approach, does not consist of the derivation of explicit unknown properties of the scaling limit. The properties it proves have been known for decades in the physics community, without, however, a proof being available. They were obtained by means of the Coulomb Gas (CG) [42] approach, and by Conformal Field Theory (CFT) [14], or Bethe Ansatz and similar techniques for integrable models [7]. Other properties were not known but can be obtained by the same methods without more difficulty.

In this chapter we give a brief description of the meaning of SLE, proofs of its basic properties, and a selection of its results (mostly without proof). For more extensive treatments and proofs, we refer the reader to several existing reviews which target different communities: Werner [54] from the mathematical perspective, Cardy [16] for physicists, and Kager e.a. [25] for both mathematicians and physicists.

A conformally invariant stochastic measure of curves naturally brings together the theory of conformal maps, stochastic calculus, and a description of curves. Already in 1923 Löwner[1] combined curves and conformal maps [39]. He considered a singly connected domain D of the complex plane (for example the upper half-plane or the unit disk) and a path $\gamma_s \in D$ starting from the boundary, and parametrized by $s > 0$. He then considered the domains D_s from which the initial part of the path is excluded: $D_s = D \setminus \gamma_{[0,s]}$. For the conformal maps that map D_s back to D he found a surprisingly simple differential equation in terms of s, provided a suitable parametrization. Schramm [46] later used this equation to define a stochastic measure of paths. It turned out that he and others could prove many properties of this measure by means of Löwner's equation.

In the following sections we will discuss some of these properties and their applications to problems in statistical physics. Though mathematical rigor is an essential ingredient of the progress made by this approach we will largely omit proofs, and rather refer the reader to the above mentioned reviews and the original literature. Only in section 3, treating the basics of SLE, do we include proofs of the various theorems.

15.2 Conformal Maps

Conformal maps play an essential role in this chapter. This is not the place to treat this subject extensively, but the notation and those few properties that are used frequently are introduced in this section. A comprehensive treatment of the subject is found in Ahlfors [1], and for a discussion more specific to SLE we refer to Kager e.a. [25] and its appendix A.

We shall write $\mathbb{C}$ for the complex plane, and $\mathbb{R}$ for the set of real numbers. The open upper half-plane $\{z : \operatorname{Im} z > 0\}$ is denoted by $\mathbb{H}$, and the open unit disk

[1] The spelling Loewner, while adopted by himself, is of later date.

$\{z : |z| < 1\}$ by $\mathbb{D}$. The defining property of conformal maps is that they preserve angles. Denoted in complex numbers this makes them holomorphic (there is no need to include the antiholomorphic variety). The basis of conformal mapping theory is the Riemann mapping theorem, which tells us that any simply connected domain D can be mapped conformally onto the open unit disk $\mathbb{D}$.

Theorem 1 (Riemann mapping theorem). *Let $D \neq \mathbb{C}$ be a simply connected domain in $\mathbb{C}$. Then there is a conformal map of D onto the open unit disk $\mathbb{D}$.*

This map is not unique, which follows from the fact that the unit disk can be conformally mapped onto itself in multiple ways, as follows from the following:

Theorem 2. *The conformal self-maps of the open unit disk $\mathbb{D}$ are precisely the transformations of the form*

$$f(z) = \mathrm{e}^{\mathrm{i}\varphi} \frac{z-a}{1-\bar{a}z}, \qquad |z| < 1, \tag{15.1}$$

where a is complex, $|a| < 1$, and $0 \leq \varphi \leq 2\pi$.

Thus it follows that the conformal map from D to $\mathbb{D}$ can be determined uniquely by three real parameters. It immediately follows that between any two singly connected domains there exists a three parameter family of conformal maps. We shall consider only domains whose boundary is a continuous curve, and this implies that the conformal maps we work with have well-defined limit values on the boundary.

Now suppose that D is a simply connected domain with a continuous boundary, and that z_1, z_2, z_3 and z_4 are distinct points on ∂D, ordered in the counter-clockwise direction. Then we can map D onto a rectangle $(0,L) \times (0,\pi)$ in such a way that the arc $[z_1, z_2]$ of ∂D maps onto $[0, \mathrm{i}\pi]$, and $[z_3, z_4]$ maps onto $[L, L+\mathrm{i}\pi]$. The length $L > 0$ of this rectangle is determined uniquely, and is called the **π-extremal distance** between $[z_1, z_2]$ and $[z_3, z_4]$ in D.

A compact subset K of $\overline{\mathbb{H}}$ such that $\mathbb{H} \setminus K$ is simply connected and $K = \overline{K \cap \mathbb{H}}$ is called a **hull** (it is basically a compact set bordering on the real line). For any hull K there exists a unique conformal map, denoted by g_K, which sends $\mathbb{H} \setminus K$ onto $\mathbb{H}$ and satisfies the normalization

$$\lim_{z \to \infty} \big(g_K(z) - z\big) = 0. \tag{15.2}$$

This map has an expansion for $z \to \infty$ of the form

$$g_K(z) = z + \frac{a_1}{z} + \ldots + \frac{a_n}{z^n} + \ldots \tag{15.3}$$

where all expansion coefficients are real. The coefficient $a_1 = a_1(K)$ is called the **capacity** of the hull K. Conformal maps that have this limit at ∞ are said to satisfy the hydrodynamic normalization.

The capacity of a nonempty hull K is a positive real number, and satisfies a **scaling rule** and a **summation rule**. The scaling rule says that if $r > 0$ then $a_1(rK) = r^2 a_1(K)$. The summation rule says that if $J \subset K$ are two hulls and L is the closure

of $g_J(K \setminus J)$, then $g_K = g_L \circ g_J$ and $a_1(K) = a_1(J) + a_1(L)$. The capacity of a hull is bounded from above by the square of the radius of the smallest half-disk that contains the hull and has its centre on the real line.

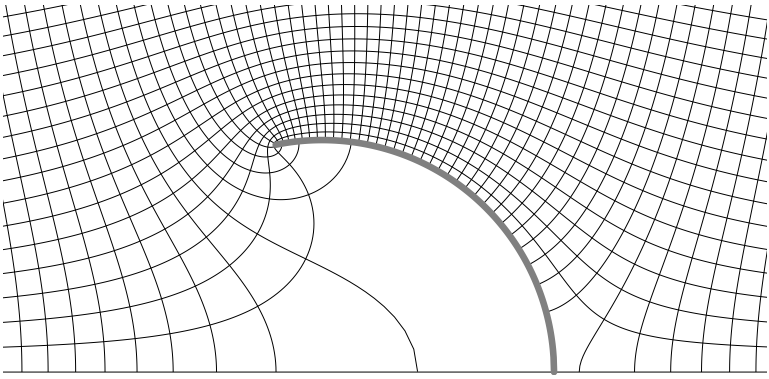

Fig. 15.1 The conformal map from $\mathbb{H}$ slit by a circular arc, to the whole of $\mathbb{H}$. The map is shown by the inverse image of the coordinate grid. The excluded arc is shown in gray.

15.3 Löwner Evolutions

In this section, we will first discuss the Löwner equation in a deterministic setting, as it was conceived by Löwner himself. Before we enter into a mathematical discussion, we will first give explicit examples of the ingredients and meaning of this celebrated equation. We will then show how one can describe a given continuous path by a family of conformal maps, and we will prove that these maps satisfy Löwner's differential equation. Then we will prove that conversely, the Löwner equation generates a family of conformal maps, that may or may not describe a continuous curve. Finally, we move on to the definition of the stochastic Löwner evolution. This section is based on ideas from Lawler, Schramm and Werner [31], Lawler [29], and Rohde and Schramm [44].

15.3.1 Describing a Path by the Löwner Equation

Suppose the upper half of the complex plane, $\mathbb{H}$, is slit by a circular arc starting at the real axis. When we exclude the points on this arc, what remains of $\mathbb{H}$ is still simply connected, provided we do not extend the arc so far that it meets the real axis again. Thus it follows that the slit upper half plane can be mapped onto the full upper half-plane by a conformal map. This map can be written in closed form, and is

shown in Fig. 15.1, by the coordinate grid of the target half plane, on the original slit half plane. The figure shows that the interior of the arc shrinks strikingly under this map. When the arc is extended so that it approaches the real axis again, the image of the interior shrinks more and more, until after closure of the arc, its interior has no image anymore.

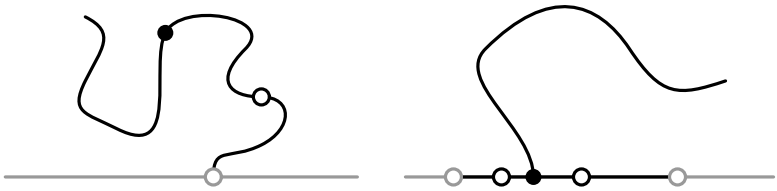

Fig. 15.2 A simple path γ_t from the origin (left). The path up to the full dot is sent to the real axis by g_t (right). The original real axis is indicated in gray, and the image of the path and its image is in black. The open point on $\gamma_{[0,t]}$ has two images under g_t.

Consider now a general simple (i.e. non-intersecting) path γ_t, in $\mathbb{H}$, parametrized by t, with $\gamma_0 = 0$, see Fig. 15.2. We choose a point $w = \gamma_t$ on the curve, indicated by a full dot, and consider the subset of the upper half-plane that excludes the part of the curve between the origin and w (or $\gamma_{[0,t]}$). Now we construct a conformal map g_t, from $\mathbb{H} \setminus \gamma_{[0,t]}$ to the entire upper half plane. Clearly since $\gamma_{[0,t]}$ are now boundary points, they are sent by g_t to the real axis. Because the curve can be approached from two sides, every point of $\gamma_{[0,t)}$ has two images on the real axis, but the image of γ_t itself is unique. Löwner discovered, that by specifying the map such that it approaches the identity at ∞, by choosing a suitable parametrization of γ_t, these conformal maps g_t satisfy the simple differential equation:

$$\frac{\partial}{\partial t} g_t(z) = \frac{2}{g_t(z) - g_t(\gamma_t)}\,, \tag{15.4}$$

which will be derived below. We note that from the definition $g_t(\gamma_t)$ is real. Thus it follows that the path γ_t can be alternately defined by the family of confomal maps g_t or by the real function $U_t \equiv g_t(\gamma_t)$. This surprising observation led Schramm to apply it to a conformally invariant measure for curves in the plane. If the probability measure of γ_t is conformally invariant, the law for $\gamma_{[0,\tau]}$ is the same as for $g_t(\gamma_{[t,t+\tau]})$. Since U_t fully determines the curve γ_t, it is pertinent to investigate the law of U_t, see subsection 15.3.3. The condition that the path is simple is unnecessary, as we shall see now in a more formal treatment.

Suppose that γ_t (where $t \geq 0$) is a continuous path in $\overline{\mathbb{H}}$ which starts from $\gamma_0 \in \mathbb{R}$. The parameter t, to be defined later, will be referred to as time. We allow the path to hit itself or the real line, but if it does, we require the path to reflect off into open space immediately. In other words, the path is not allowed to enter a region which has been disconnected from infinity by $\gamma_{[0,t]} \cup \mathbb{R}$. To be specific, let us denote by H_t

for $t \geq 0$ the unbounded connected component of $\mathbb{H} \setminus \gamma_{[0,t]}$, and let K_t be the closure of $\mathbb{H} \setminus H_t$. Then we require that for all $0 \leq s < t$, K_s is a proper subset of K_t. See Fig. 15.3 for a picture of a path satisfying these conditions.

We further impose the conditions that for all $t \geq 0$ the set K_t is bounded, so that $\{K_t : t \geq 0\}$ is a family of growing hulls, and that the capacity of these hulls eventually goes to infinity, i.e. $\lim_{t\to\infty} a_1(K_t) = \infty$. The latter condition implies that the path eventually has to escape to infinity (this is a necessary but not sufficient condition for the hull to diverge, see e.g. section A.4 of [25]). Now let us state the purpose of this subsection.

For every $t \geq 0$ we set $g_t := g_{K_t}$, and we further define the real-valued function $U_t := g_t(\gamma_t)$ (this is the point to which the tip of the path is mapped). The purpose of this subsection is to prove that the maps g_t satisfy a simple differential equation, which is 'driven' by U_t. Ideas for the proof were taken from [31]. For a different, probabilistic approach, see [29]. The first thing that we show, is that we can choose the time parameterization of γ such that the capacity grows linearly in time. Clearly, this fact is a direct consequence of the following theorem.

Theorem 3. *Both $a_1(K_t)$ and U_t are continuous in t.*

Proof. The proof relies heavily on properties of π-extremal distance, and we refer to the chapter on extremal length, sections 4.1–4.5 and 4.11–4.13, in Ahlfors [1] for the details. We shall prove left-continuity first.

Without loss of generality we may assume that $\gamma_0 = 0$. Fix $t > 0$, let R be a large number, say at least several times the radius of K_t, and let C_R be the upper half of the circle with radius $2R$ centred at the origin. Fix $\varepsilon > 0$. Then by continuity of γ_t, there exists a $\delta > 0$ such that $|\gamma_t - \gamma_u| < \varepsilon/2$ for all $u \in (t-\delta, t)$. Now let C_ε be the circle with radius ε and centre γ_t, and let S be the arc of this circle in the domain H_t. Then this set S disconnects $K_t \setminus K_{t-\delta}$ from infinity in $H_{t-\delta}$, see Fig. 15.3. Observe that the set $K_t \setminus K_{t-\delta}$ may be just a piece of γ, but that it can also be much larger, as in the figure.

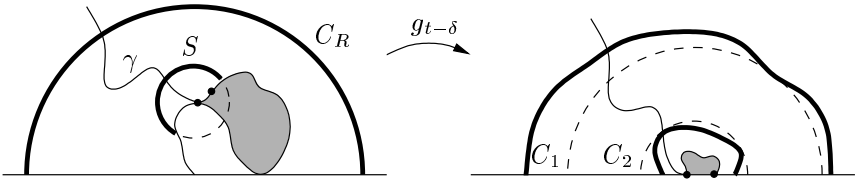

Fig. 15.3 A path γ. The two points represent γ_t and $\gamma_{t-\delta}$, and the shaded area is the set $K_t \setminus K_{t-\delta}$. For clarity, the arc C_R is drawn much smaller than it is in the proof.

For convenience let us denote by Ω the part of the domain $H_{t-\delta}$ that lies below C_R. Let $\mathscr{L}$ be the π-extremal distance between S and C_R in Ω. By the properties of π-extremal distance, because the circle with radius R and centre at γ_t lies below C_R, $\mathscr{L}$ must be at least $\log(R/\varepsilon)/2$. Note that since π-extremal distance is in-

variant under conformal maps, $\mathscr{L}$ is also the π-extremal distance between $g_{t-\delta}(C_R)$ and $g_{t-\delta}(S)$ in $g_{t-\delta}(\Omega)$. This allows us to find an upper bound on $\mathscr{L}$.

To get this upper bound, we draw two concentric semi-circles C_1 and C_2, the first hitting $g_{t-\delta}(C_R)$ on the inside, and the second hitting $g_{t-\delta}(S)$ on the outside as in Fig. 15.3 (this is always possible if R was chosen large enough). Note that by the hydrodynamic normalization of the map $g_{t-\delta}$, we have an upper bound on the radius of C_1, which depends only on R. As is explained in Ahlfors, this means that the π-extremal distance $\mathscr{L}$ satisfies an inequality of the form $\mathscr{L} \leq \log(C(R)/r)$, where $C(R)$ depends only on our choice of R, and r is the radius of the inner half-circle C_2. But $\mathscr{L}$ was at least $\log(R/\varepsilon)/2$, implying that r can be made arbitrarily small by choosing δ small enough. It follows that for every $\varepsilon > 0$ there exists a $\delta > 0$ such that the set $K_{t,\delta} := g_{t-\delta}(K_t \setminus K_{t-\delta})$ is contained in a half-disk of radius ε. But then by the summation rule of capacity $a_1(K_t) - a_1(K_{t-\delta}) = a_1(K_{t,\delta}) \leq \varepsilon^2$, proving left-continuity of $a_1(K_t)$.

To prove left-continuity of U_t, let δ and ε be as above, and denote by $g_{t,\delta}$ the normalized map $g_{K_{t,\delta}}$ associated with the hull $K_{t,\delta}$. It is clearly sufficient to show that $g_{t,\delta}$ converges uniformly to the identity as $\delta \downarrow 0$ (remember that U_t is defined as $g_t(\gamma_t)$ and refer to Fig. 15.3). To prove this, we may assume without loss of generality that the set $K_{t,\delta}$ is contained within the disk of radius ε centred at the origin, since the claim remains valid under translations over the real line. But for a hull bounded within a radius ε the n-th order coefficient of the asymptotic expansion of g_t is bounded by ε^{n+1} (see equation (A.11) in [25]). Therefore, for $|z| > 2\varepsilon$,

$$|g_{t,\delta}(z) - z| \leq \sum_{n=1}^{\infty} \frac{a_n(K_{t,\delta})}{|z|^n} \leq \varepsilon \sum_{n=1}^{\infty} \frac{\varepsilon^n}{(2\varepsilon)^n} = \varepsilon. \tag{15.5}$$

This shows that the map $g_{t,\delta}$ converges uniformly to the identity. Left-continuity of U_t follows. In the same way we can prove right-continuity of $a_1(K_t)$ and U_t.

Theorem 4. *Let γ_t be parameterized such that $a_1(K_t) = 2t$. Then for all $z \in \mathbb{H}$, as long as z is not an element of the growing hull, $g_t(z)$ satisfies the Löwner differential equation*

$$\frac{\partial}{\partial t} g_t(z) = \frac{2}{g_t(z) - U_t}, \quad g_0(z) = z. \tag{15.6}$$

Proof. Our proof is based on the proof of theorem 3 and the Poisson integral formula, which states that the map $g_{t,\delta}$ satisfies

$$g_{t,\delta}(z) - z = \frac{1}{\pi} \int_{-\infty}^{\infty} \frac{\operatorname{Im} g_{t,\delta}^{-1}(\xi)}{g_{t,\delta}(z) - \xi} \, \mathrm{d}\xi, \qquad z \in \mathbb{H} \setminus K_{t,\delta} \tag{15.7}$$

while the capacity $a_1(K_{t,\delta})$ is given by the integral

$$a_1(K_{t,\delta}) = \frac{1}{\pi} \int_{-\infty}^{\infty} \operatorname{Im} g_{t,\delta}^{-1}(\xi) \, \mathrm{d}\xi. \tag{15.8}$$

First consider the left-derivative of $g_t(z)$. Using the same notation as in the proof of theorem 3 we can write $g_t = g_{t,\delta} \circ g_{t-\delta}$. We know that $g_{t,\delta}$ converges to the identity as $\delta \downarrow 0$, and that the support of $\operatorname{Im} g_{t,\delta}^{-1}$ on the real line shrinks to the point U_t. Moreover, using the summation rule of capacity and our choice of time parameterization, equation (15.8) gives $\int \operatorname{Im} g_{t,\delta}^{-1}(\xi)\,\mathrm{d}\xi = 2\pi\delta$. Hence from equation (15.7) we get

$$\lim_{\delta\downarrow 0} \frac{g_t(z) - g_{t-\delta}(z)}{\delta} = \lim_{\delta\downarrow 0} \frac{1}{\pi\delta} \int \frac{\operatorname{Im} g_{t,\delta}^{-1}(\xi)}{g_{t,\delta}\big(g_{t-\delta}(z)\big) - \xi}\,\mathrm{d}\xi = \frac{2}{g_t(z) - U_t}. \tag{15.9}$$

In the same way one obtains the right-derivative.

15.3.2 The Solution of the Löwner Equation

In the previous subsection, we started from a continuous path γ in the upper half-plane. We proved that the corresponding conformal maps satisfy the Löwner equation, driven by a suitably defined continuous function U_t. In this subsection, we will try to go the other way around. Starting from a driving function U_t, we will prove that the Löwner equation generates a (continuous) family of conformal maps g_t onto $\mathbb{H}$. The proof follows Lawler [29].

So suppose that we have a continuous real-valued function U_t. Consider for some point $z \in \overline{\mathbb{H}} \setminus \{0\}$ the Löwner differential equation

$$\frac{\partial}{\partial t} g_t(z) = \frac{2}{g_t(z) - U_t}, \qquad g_0(z) = z. \tag{15.10}$$

This equation gives us some immediate information on the behaviour of $g_t(z)$. For instance, taking the imaginary part we obtain

$$\frac{\partial}{\partial t} \operatorname{Im} g_t(z) = \frac{-2 \operatorname{Im} g_t(z)}{(\operatorname{Re} g_t(z) - U_t)^2 + (\operatorname{Im} g_t(z))^2}. \tag{15.11}$$

This shows that for fixed $z \in \mathbb{H}$, $\partial_t \operatorname{Im}[g_t(z)] < 0$, and hence that $g_t(z)$ moves towards the real axis. Further, points on the real axis will stay on the real axis.

For a given point $z \in \overline{\mathbb{H}} \setminus \{0\}$, the solution of the Löwner equation is well-defined as long as $g_t(z) - U_t$ stays away from zero. This suggests that we define a time $\tau(z)$ as the first time τ such that $\lim_{t\uparrow\tau}(g_t(z) - U_t) = 0$, setting $\tau(z) = \infty$ if this never happens. Note that as long as $g_t(z) - U_t$ is bounded away from zero, equation (15.11) shows that the time derivative of $\operatorname{Im}[g_t(z)]$ is bounded in absolute value by some constant times $\operatorname{Im}[g_t(z)]$. For points $z \in \mathbb{H}$ this shows that in fact, $\tau(z)$ must be the first time when $g_t(z)$ hits the real axis. We set

$$H_t := \{z \in \mathbb{H} : \tau(z) > t\}, \qquad K_t := \{z \in \overline{\mathbb{H}} : \tau(z) \le t\}. \tag{15.12}$$

Then H_t is the set of points in the upper half-plane for which $g_t(z)$ is still well-defined, and K_t is the closure of its complement, i.e. it is the hull which is excluded from H_t. Our goal is now to prove the following theorem.

Theorem 5. *Let U_t be a continuous real-valued function, and for every $t \geq 0$ let $g_t(z)$ be the solution of the Löwner equation (15.10). Define the set H_t as in (15.12). Then $g_t(z)$ is a conformal map of the domain H_t onto $\mathbb{H}$ which satisfies*

$$g_t(z) = z + \frac{2t}{z} + O\left(z^{-2}\right), \qquad z \to \infty. \tag{15.13}$$

Proof. It is easy to see from (15.10) that g_t is analytic on H_t. We will prove (i) that the map g_t is conformal on the domain H_t, (ii) that this map is of the form (15.13), and (iii) that $g_t(H_t) = \mathbb{H}$.

To prove (i), we have to verify that g_t has non-zero derivative on H_t, and that it is injective. So consider equation (15.10) for times $t < \tau(z)$. Then the differential equation behaves nicely, and we can differentiate with respect to z to obtain

$$\frac{\partial}{\partial t} \log g_t'(z) = -\frac{2}{(g_t(z) - U_t)^2}. \tag{15.14}$$

This gives $|\partial_t \log g_t'(z)| \leq 2/[\operatorname{Im} g_t(z)]^2$. But we know that $\operatorname{Im}[g_t(z)]$ is decreasing. Hence, if we fix $t_0 < \tau(z)$, then the change in $\log g_t'(z)$ is uniformly bounded for all times $t < t_0$. It follows that $\log g_{t_0}'(z)$ is well-defined and bounded and hence, that $g_t'(z)$ is well-defined and non-zero for all $t < \tau(z)$.

Next, choose two different points $z, w \in \mathbb{H}$ and let $t < \min\{\tau(z), \tau(w)\}$. Then

$$\frac{\partial}{\partial t} \log[g_t(z) - g_t(w)] = -\frac{2}{(g_t(z) - U_t)(g_t(w) - U_t)}. \tag{15.15}$$

It follows that $g_t(z) \neq g_t(w)$ for all $t < \min\{\tau(z), \tau(w)\}$, using a similar argument as above. We conclude that $g_t(z)$ is conformal on the domain H_t.

For the proof of (ii), we note that (i) implies that the map $g_t(z)$ can be expanded around infinity. We can determine the form of the expansion by integrating the Löwner differential equation from 0 to t. This yields

$$g_t(z) - z = \int_0^t \frac{2\mathrm{d}s}{g_s(z) - U_s}. \tag{15.16}$$

Consider this equation in the limit $z \to \infty$. Then it is easy to see that the expansion of $g_t(z)$ has no terms of quadratic or higher power in z, and no constant term. The form (15.13) follows immediately.

Finally, we prove (iii), i.e. we will show that $g_t(H_t) = \mathbb{H}$. To see this, let w be any point in $\mathbb{H}$, and let t_0 be a fixed time. Define $h_t(w)$ for $0 \leq t \leq t_0$ as the solution of the problem

$$\frac{\partial}{\partial t} h_t(w) = -\frac{2}{h_t(w) - U_{t_0 - t}}, \qquad h_0(w) = w. \tag{15.17}$$

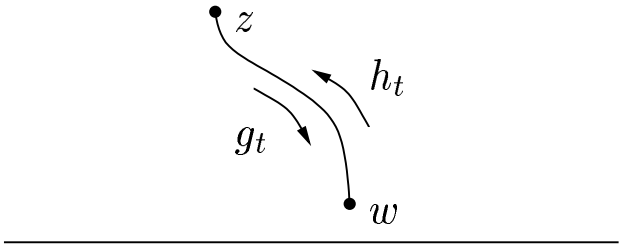

Fig. 15.4 If the flow of a point z up to a time t_0 is described by $g_t(z)$, then $h_t(w)$ as defined in the text describes the inverse flow.

The imaginary part of this equation says that $\partial_t \operatorname{Im}[h_t(w)] > 0$ and hence, that $\operatorname{Im}[h_t(w)]$ is increasing in time. Since $|\partial_t h_t(w)| \leq 2/\operatorname{Im}[h_t(w)]$, it follows that $h_t(w)$ is well-defined for all $0 \leq t \leq t_0$.

We defined $h_t(w)$ such that it describes the inverse of the flow of some point $z \in H_{t_0}$ under the Löwner evolution (15.10) (see Fig. 15.4). To see that this is indeed the case, suppose that for some t between 0 and t_0, $h_{t_0-t}(w) = g_t(z)$ for some z. Then it follows from the differential equation for $h_t(w)$, that $g_t(z)$ satisfies equation (15.10). This observation holds for all times t between 0 and t_0. It follows that such a point z exists, and that it is in fact determined by $z = g_0(z) = h_{t_0}(w)$. In other words, for all $w \in \mathbb{H}$ we have $g_{t_0}(z) = w$ for some $z \in H_{t_0}$. This completes the proof.

We have just proved that a continuous function U_t leads, via the Löwner evolution equation (15.10), to a collection of conformal maps $\{g_t : t \geq 0\}$. These conformal maps are defined on subsets of the upper half-plane, namely the sets $H_t = \mathbb{H} \setminus K_t$, with K_t a growing hull. At this point we still don't know if the maps $g_t(z)$ also correspond to a path γ_t. But in the next subsection we shall take U_t to be a scaled Brownian motion, and it is known [44] that in this case the Löwner evolution does correspond to a path.

In a few cases the solution of the Löwner equation for γ_t and U_t, the pair of a path and its corresponding driving term, is known [24]. To find such solutions one may choose a form of U_t, so that Löwner's equation can be solved. An alternative is to find paths γ_t for which the conformal map g_t is known, and simply calculate U_t from the Löwner equation. Kager e.a. [24] calculated the traces γ_t for the cases U_t constant, linearly dependent on t and proportional to $t^{1/2}$ and to $(1-t)^{1/2}$. In the last case the behavior depends critically on the prefactor of the driving term: for small coefficient the path spirals in to a point in $\mathbb{H}$, and for large coefficient the path ends on the real axis.

15.3.3 Chordal SLE in the Half-Plane

In the previous subsection we showed that the Löwner equation (15.10) driven by a continuous real-valued function generates a set of conformal maps. Furthermore, these conformal maps may correspond to a path in the upper half-plane, as is suggested by the conclusions of section 15.3.1. Chordal SLE_κ in the half-plane is obtained by taking scaled Brownian motion as the driving process. We give a precise definition in this subsection.

Let B_t, $t \in [0,\infty)$, be a standard Brownian motion on $\mathbb{R}$, starting from $B_0 = 0$, and let $\kappa > 0$ be a real parameter. For each $z \in \overline{\mathbb{H}} \setminus \{0\}$, consider the Löwner differential equation

$$\frac{\partial}{\partial t} g_t(z) = \frac{2}{g_t(z) - \sqrt{\kappa} B_t}, \quad g_0(z) = z. \tag{15.18}$$

This has a solution as long as the denominator $g_t(z) - \sqrt{\kappa} B_t$ stays away from zero.

For all $z \in \overline{\mathbb{H}}$, just as in the previous subsection, we define $\tau(z)$ to be the first time τ such that $\lim_{t \uparrow \tau} (g_t(z) - \sqrt{\kappa} B_t) = 0$, and $\tau(z) = \infty$ if this never happens, and we set

$$H_t := \{z \in \mathbb{H} : \tau(z) > t\}, \qquad K_t := \{z \in \overline{\mathbb{H}} : \tau(z) \le t\}. \tag{15.19}$$

That is, H_t is the set of points in the upper half-plane for which $g_t(z)$ is well-defined, and $H_t = \mathbb{H} \setminus K_t$. The definition is such that K_t is a hull, while H_t is a simply-connected domain. We showed in the previous subsection that for every $t \ge 0$, g_t defines a conformal map of H_t onto the upper half-plane $\mathbb{H}$, that satisfies the normalization $\lim_{z \to \infty} (g_t(z) - z) = 0$.

Definition 1 (Stochastic Löwner Evolution). The family of conformal maps $\{g_t : t \ge 0\}$ defined through the stochastic Löwner equation (15.18) is called **chordal SLE_κ**. The sets K_t (15.19) are the **hulls** of the process.

The SLE_κ process defined through equation (15.18) is called chordal, because its hulls are growing from a point on the boundary (the origin) to another point on the boundary (infinity). We will keep using the term chordal for processes going between two boundary points (and not only for SLE processes). Other kinds of processes might for instance grow from a point on the boundary to a point in the interior of a domain. An example of such a process is radial SLE, see section 15.3.5.

It turns out that the hulls of chordal SLE in fact are the hulls of a continuous path γ_t, that is called the **trace** of the SLE process. It is through this trace that the connection with discrete models can be made. We shall discuss properties of the trace in section 15.4, and we will look at the connection with discrete models in section 15.5. The precise definition of the trace is as follows.

Definition 2 (Trace). The **trace** γ of SLE_κ is defined by

$$\gamma_t := \lim_{z \to 0} g_t^{-1}(z + \sqrt{\kappa} B_t), \tag{15.20}$$

where the limit is taken from within the upper half-plane.

At this point we would like to make some remarks about the choice of time parameterization. Chordal SLE is defined such that the capacity of the hull K_t satisfies $a_1(K_t) = 2t$, and this may seem somewhat arbitrary. But in practice, the choice of time parameterization does not matter for our calculations. The point is, that in SLE calculations we are usually interested in expectated values of random variables at the first time when some event happens, that is, at a stopping time. These values are clearly independent from the chosen time parameterization (even if we make a random change of time). For examples of such calculations, see sections 15.4.2 and 15.6.1.

Still, it is interesting to examine how a time-change affects the Löwner equation. So, let $c(t)$ be an increasing and differentiable function defining a change of time. Then $\hat{g}_t := g_{c(t)/2}$ is a collection of conformal transformations parameterized such that $a_1(\hat{K}_t) := a_1(K_{c(t)/2}) = c(t)$. This family of transformations satisfies the equation

$$\frac{\partial}{\partial t}\hat{g}_t(z) = \frac{\frac{\mathrm{d}}{\mathrm{d}t}c(t)}{\hat{g}_t(z) - \sqrt{k}B_{c(t)/2}}, \qquad \hat{g}_0(z) = z. \tag{15.21}$$

In particular, if we choose $c(t) = 2\alpha t$ for some constant $\alpha > 0$, then the conformal maps $\hat{g}_t$ satisfy

$$\frac{\partial}{\partial t}\frac{1}{\sqrt{\alpha}}\hat{g}_t(\sqrt{\alpha}z) = \frac{2}{\frac{1}{\sqrt{\alpha}}\hat{g}_t(\sqrt{\alpha}z) - \sqrt{\frac{\kappa}{\alpha}}B_{\alpha t}}, \qquad \frac{1}{\sqrt{\alpha}}\hat{g}_0(\sqrt{\alpha}z) = z. \tag{15.22}$$

But the scaling property of Brownian motion shows that the driving term of this Löwner equation is again a standard Brownian motion multiplied by $\sqrt{\kappa}$. This proves the following lemma.

Lemma 1 (Scaling property of SLE$_\kappa$). *If g_t are the transformations of SLE$_\kappa$ and α is a positive constant, then the process $(t,z) \mapsto \hat{g}_t(z) := \alpha^{-1/2} g_{\alpha t}(\sqrt{\alpha}z)$ has the same distribution as the process $(t,z) \mapsto g_t(z)$. Furthermore, the process $t \mapsto \alpha^{-1/2}K_{\alpha t}$ has the same distribution as the process $t \mapsto K_t$.*

This lemma is used frequently in SLE calculations. Its significance will be shown already in the following subsection, where we define the SLE$_\kappa$ process in an arbitrary simply connected domain. Meanwhile, the strong Markov property of Brownian motion implies that chordal SLE$_\kappa$ has another basic property, which is referred to as stationarity. Indeed, for any stopping time τ the process $\sqrt{\kappa}(B_{t+\tau} - B_\tau)$ is itself a standard Brownian motion multiplied by $\sqrt{\kappa}$. So if we use this process as a driving term in the Löwner equation, we will obtain a collection of conformal maps $\hat{g}_t$ which is equal in distribution to the normal SLE$_\kappa$ process.

It is not difficult to see that the process $\hat{g}_t(z)$ in question is in fact the process defined by

$$\hat{g}_t(z) := g_{t+\tau}\left(g_\tau^{-1}(z + \sqrt{\kappa}B_\tau)\right) - \sqrt{\kappa}B_\tau. \tag{15.23}$$

Indeed, taking the derivative of $\hat{g}_t(z)$ with respect to t, we find that this process satisfies the Löwner equation

$$\frac{\partial}{\partial t}\hat{g}_t(z) = \frac{2}{\hat{g}_t(z) - \sqrt{\kappa}(B_{t+\tau} - B_\tau)}, \qquad \hat{g}_0(z) = z. \tag{15.24}$$

This result establishes the following lemma.

Lemma 2 (Stationarity of SLE$_\kappa$). *Let $g_t(z)$ be an SLE$_\kappa$ process in $\mathbb{H}$, and let τ be a stopping time. Define $\hat{g}_t(z)$ by (15.23). Then $\hat{g}_t$ has the same distribution as g_t, and it is independent from $\{g_t : t \in [0,\tau]\}$.*

Observe that the process $\hat{g}_t$ of this lemma is just the original SLE$_\kappa$ process from the time τ onwards, but shifted in such a way that the new process starts again in the origin. The content of the lemma is that this new process is the same in distribution as the standard SLE$_\kappa$ process, and independent from the history up to time τ. So it is in this sense that the SLE$_\kappa$ process is stationary.

15.3.4 Chordal SLE in an Arbitrary Domain

Suppose that $D \subsetneq \mathbb{C}$ is a simply connected domain. Then the Riemann mapping theorem says that there is a conformal map $f : D \to \mathbb{H}$. Now, let f_t be the solution of the Löwner equation (15.18) with initial condition $f_0(z) = f(z)$ for $z \in D$. Then we will call the process $\{f_t : t \geq 0\}$ the SLE$_\kappa$ in D under the map f. The connection with the solution g_t of (15.18), with initial condition $g_0(z) = z$, is easily established. Obviously we have $f_t = g_t \circ f$, and if K_t are the hulls associated with g_t, then the hulls associated with f_t are $f^{-1}(K_t)$.

Now suppose that we want to consider an SLE$_\kappa$ trace that crosses some domain D from a specified point $a \in \partial D$ to another specified point $b \in \partial D$, $a \neq b$. Then we can find a conformal map $f : D \to \mathbb{H}$ such that $f(a) = 0$ and $f(b) = \infty$. The SLE$_\kappa$ process from a to b in D under the map f is then defined as we discussed above, with starting point $f(a) = 0$.

The map f, however, is not determined uniquely. But the maps $\tilde{f}$ of D onto $\mathbb{H}$ that sends a to 0 and b to ∞, have only one free parameter (see section 15.2), scaling the whole map: $\tilde{f}(z) = \alpha f(z)$.

Lemma 1 then tells us that the trace of the SLE$_\kappa$ process in D under $\tilde{f}$ is given simply by a linear time-change of the SLE$_\kappa$ process under f. But we explained in the previous subsection that a time-change does not affect our calculations, and may therefore be ignored. Hence, in the sequel, we can simply speak of SLE processes in an arbitrary domain, without mentioning the conformal maps that take these processes to the upper half-plane.

15.3.5 Radial SLE

So far we have looked only at chordal Löwner evolution processes, which grow from one point on the boundary of a domain to another point on the boundary. One can also study Löwner evolution processes which grow from a boundary point to a point in the interior of the domain. These are known as **radial** Löwner evolutions. Radial SLE_κ in the unit disk, for example, is defined as follows.

Let B_t again be Brownian motion, and $\kappa > 0$. Set $W_t := \exp(\mathrm{i}\sqrt{\kappa}B_t)$, so that W_t is Brownian motion on the unit circle starting from 1. Then radial SLE_κ is defined to be the solution of the Löwner equation

$$\frac{\partial}{\partial t} g_t(z) = g_t(z) \frac{W_t + g_t(z)}{W_t - g_t(z)}, \quad g_0(z) = z, \quad z \in \overline{\mathbb{D}}. \tag{15.25}$$

The solution again exists up to a time $\tau(z)$ which is defined to be the first time τ such that $\lim_{t\uparrow\tau}(g_t(z) - W_t) = 0$.

If we set

$$H_t := \{z \in \mathbb{D} : \tau(z) > t\}, \qquad K_t := \{z \in \overline{\mathbb{D}} : \tau(z) \le t\}, \tag{15.26}$$

then g_t is a conformal map of $\mathbb{D} \setminus K_t = H_t$ onto $\mathbb{D}$. The maps are in this case normalized by $g_t(0) = 0$ and $g_t'(0) > 0$. In fact it is easy to see from the Löwner equation that $g_t'(0) = \exp(t)$, and this specifies the time parameterization.

The trace of radial SLE_κ is defined by $\gamma_t := \lim_{z\to W_t} g_t^{-1}(z)$, where now the limit is to be taken from within the unit disk. The trace goes from the starting point 1 on the boundary to the origin. By conformal mappings, one can likewise define radial SLE in an arbitrary simply connected domain, growing from a given point on the boundary to a given point in the interior.

15.3.6 Dipolar SLE

A third version of the SLE process is one that can terminate anywhere on a singly connected segment of the boundary. This process is called dipolar SLE [6]. Consider a domain D with three boundary points, x_-, x_0, and x_+, with $x_0 \in (x_-, x_+)$. We consider paths γ_t with $\gamma_0 = x_0$ terminating in the interval (x_+, x_-). The conformal map g_t sends $\gamma_{[0,t]}$ to the interval (x_-, x_+). It leaves x_- and x_+ invariant and satisfies $g_t'(x_-) = g_t'(x_+)$. The domain in which the defining equation is simplest is the strip $\mathbb{S} = \{z \in \mathbb{C} : 0 < \mathrm{Im}\, z < 2\pi\}$. The two boundary fixed points are $x_\pm = \pm\infty$ and the starting point $x_0 = 0$:

$$\partial_t g_t(z) = \frac{2}{\tanh\left(g_t(z) - \sqrt{\kappa}B_t\right)}, \tag{15.27}$$

with $g_0(z) = z$ and $z \in \mathbb{S}$. Generalized versions of SLE called $\mathrm{SLE}_{\kappa,\rho}$ [38, 56] have been constructed, in which the driving term contains a drift with respect to special points on the boundary. This review will not be concerned with this generalization.

15.4 Properties of SLE

So far we have not said very much about the parameter κ. At first sight it looks very innocent, as it scales only the parameter t. It can not, however, be eliminated from Löwner's equation, which indicates that it may not be as ineffectual as it seems. In the deterministic context the behavior depends in a qualitative way on the prefactor of the driving term (end of subsection 15.3.2 and [24]), when the driving term has a square-root singularity. This convincingly contradicts the naive intuition that the prefactor κ in (15.18) is irrelevant. In this section we show how SLE_κ depends qualitatively on its index.

First we shall see that the family of conformal maps $\{g_t : t \geq 0\}$ that is the solution of the stochastic Löwner equation (15.18) does describe a continuous path. We will look at the properties of this path, and we shall describe the connection with the hulls $\{K_t : t \geq 0\}$ of the process. All of this work was done originally by Rohde and Schramm [44]. We shall also see that SLE has some special properties in the cases $\kappa = 6$ (locality) and $\kappa = 8/3$ (restriction), as was shown in [31] and [38]. We end the section by giving the Hausdorff dimensions of the SLE paths, calculated by Beffara [11, 10].

15.4.1 Continuity and Transience

In section 15.3.2 we proved that the solution of the Löwner equation is a family of conformal maps onto the half-plane. We then raised the question whether these conformal maps describe a continuous path. Rohde and Schramm [44] proved that for chordal SLE_κ this is indeed the case, at least for all $\kappa \neq 8$. The proof by Rohde and Schramm does not work for $\kappa = 8$. But later, Lawler, Schramm and Werner [36] proved that SLE_8 is the scaling limit of the Peano curve winding around a uniform spanning tree (more details follow in section 15.5). Thereby, they showed indirectly that the trace is a continuous curve in the case $\kappa = 8$ as well. More precisely, the following theorem holds.

Theorem 6 (Continuity). *For all $\kappa \geq 0$ almost surely the limit*

$$\gamma_t := \lim_{z \to 0} g_t^{-1}(z + \sqrt{\kappa} B_t) \tag{15.28}$$

exists for every $t \geq 0$, where the limit is taken from within the upper half-plane. Moreover, almost surely $\gamma : [0,\infty) \to \overline{\mathbb{H}}$ is a continuous path and H_t is the unbounded connected component of $\mathbb{H} \setminus \gamma_{[0,t]}$ for all $t \geq 0$.

In the same paper, Rohde and Schramm also showed that the trace of SLE_κ is transient for all $\kappa \geq 0$, that is, $\lim_{t\to\infty} |\gamma_t| = \infty$ almost surely. This proves that the SLE process in the half-plane is indeed a chordal process growing from 0 to infinity.

15.4.2 Phases of SLE

The behaviour of the trace of SLE_κ depends naturally on the value of the parameter κ. It is the purpose of this subsection to point out that we can discern three different phases in the behaviour of this trace. The two phase transitions take place at the values $\kappa = 4$ and $\kappa = 8$. A sketch of what the three different phases look like is given in Fig. 15.5.

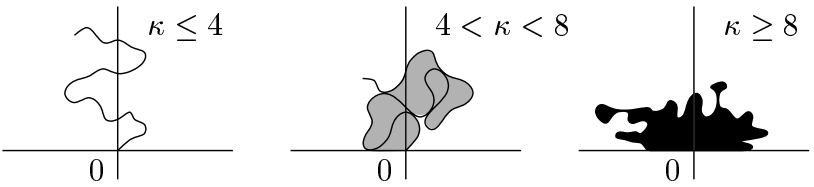

Fig. 15.5 Simplified impression of SLE in the three different phases. The trace of the SLE process is shown in black. The union of the black path and the grey areas represents the hull.

For $\kappa \in [0,4]$ the SLE_κ trace γ is almost surely a simple path, i.e. $\gamma_s \neq \gamma_t$ for all $0 \leq t < s$. Moreover, the trace a.s. does not hit the real line but stays in the upper half-plane after time 0. Clearly then, the hulls K_t of the process coincide with the trace $\gamma_{[0,t]}$.

When κ is larger than 4, the trace is no longer simple. In fact, for all $\kappa > 4$ every point $z \in \overline{\mathbb{H}} \setminus \{0\}$ a.s. becomes part of the hull in finite time. This means that every point is either on the trace, or is disconnected from infinity by the trace. But as long as $\kappa < 8$, it can be shown that the former happens with probability zero. Therefore, for $\kappa \in (4,8)$ we have a phase where the trace is not dense but does eventually disconnect all points from infinity. In other words, the trace now intersects both itself and the real line, and the hulls K_t now consist of the union of the trace $\gamma_{[0,t]}$ and all bounded components of $\overline{\mathbb{H}} \setminus \gamma_{[0,t]}$.

Finally, when $\kappa \geq 8$ the trace becomes dense in $\mathbb{H}$. In fact, we are then in a phase where $\gamma_{[0,\infty)} = \overline{\mathbb{H}}$ with probability 1, and the hulls K_t coincide with the trace $\gamma_{[0,t]}$ again.

15.4.3 Locality and Restriction

We discussed above the two special values of κ, 4 and 8, where SLE undergoes a phase transition. Two other special values of κ, $\kappa = 6$ and $\kappa = 8/3$, have received much attention from the beginning. At these values, SLE_κ has some very specific properties, that will be discussed in detail below.

15.4.3.1 The Locality Property of SLE_6

Let us start by giving a precise definition of the locality property. Assume for now that $\kappa > 0$ is fixed. Suppose that L is a hull in $\mathbb{H}$ which is bounded away from the origin. Let K_t be the hulls of a chordal SLE_κ process in $\mathbb{H}$, and let K_t^* be the hulls of a chordal SLE_κ process in $\mathbb{H} \setminus L$, both processes going from 0 to ∞. Denote by T_L the first time at which K_t intersects the set L. Likewise, let T_L^* be the first time when K_t^* intersects L (note that in this case, T_L^* is the hitting time of an arc on the boundary of the domain). See Fig. 15.6 for an illustration comparing the traces of the two processes in their respective domains.

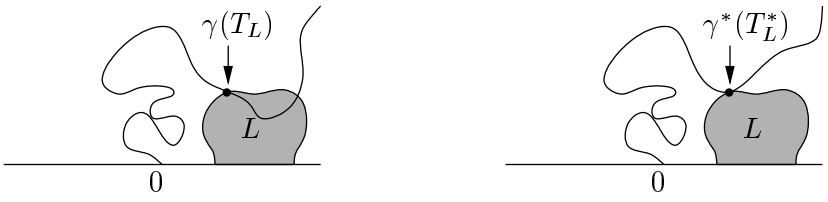

Fig. 15.6 Comparison of two SLE_κ processes from 0 to ∞, in the domain $\mathbb{H}$ (left) and in the domain $\mathbb{H} \setminus L$ (right). If these processes have the same distribution up to the hitting time of the set L, then we say that SLE_κ has the locality property.

Chordal SLE_κ is said to satisfy the locality property if for all hulls L bounded away from the origin, the distribution of the hulls $\{K_t : t < T_L\}$ is the same as the distribution of the hulls $\{K_t^* : t < T_L^*\}$, modulo a time re-parameterization. Loosely speaking, suppose that SLE_κ has the locality property, and that we are only interested in the process up to the first time that it hits L. Then it doesn't matter whether we consider chordal SLE_κ from 0 to ∞ in the domain $\mathbb{H}$, or in the smaller domain $\mathbb{H} \setminus L$. Because the equivalence between these processes may involve a time reparametrization, the hitting times T_L and T_L^* need not be the same, but all the hulls in $\{K_t : t < T_L\}$ appear in $\{K_t^* : t < T_L^*\}$ in the same order.

It was first proved in [31] that chordal SLE_κ has the locality property for $\kappa = 6$, and for no other values of κ. Later, a much simpler proof appeared in [38]. A sketch of the proof with a discussion of some consequences appears in [29].

So far, we defined the locality property for a chordal process in $\mathbb{H}$, but it is clear that by conformal invariance (invariance under conformal maps) we can translate

the property to an arbitrary simply connected domain. It is also true that radial and dipolar SLE_6 have the same property. We shall not go into this further, but we would like to point out one particular consequence of the locality property of SLE_6.

Suppose that D is a simply connected domain with continuous boundary, and let a, b and b' be three distinct points on the boundary of D. Denote by I the arc of ∂D between b and b' which does not contain a (see Fig. 15.7 for an illustration). Let K_t (respectively K'_t) be the hulls of a chordal SLE_6 process from a to b (respectively b') in D, and let T (respectively T') be the first time when the process hits I. Then modulo a time-change, $\{K_t : t < T\}$ and $\{K'_t : t < T'\}$ have the same distribution. As a result, the hulls of dipolar SLE_6 are the same as those of chordal SLE_6 up to the time the exit arc of the dipolar process is hit.

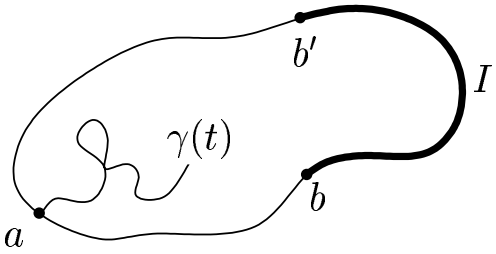

Fig. 15.7 An SLE_κ process aimed towards an arc I on the boundary of a domain.

15.4.3.2 The Restriction Property of $\mathrm{SLE}_{8/3}$

To define the restriction property, assume that $\kappa \leq 4$ is fixed. Then the trace γ of SLE_κ is a simple path. Now suppose, as in our discussion of the locality property above, that L is a hull in the half-plane which is bounded away from the origin. Let Ψ be the map defined by $\Psi(z) := g_L(z) - g_L(0)$. Then Ψ is the unique conformal map of $\mathbb{H} \setminus L$ onto $\mathbb{H}$ such that $\Psi(0) = 0$, $\Psi(\infty) = \infty$ and $\Psi'(\infty) = 1$. Now suppose that γ never hits L. Then we let γ^* be the image of γ under the map Ψ, that is $\gamma^*_t := \Psi(\gamma_t)$.

We say that SLE_κ has the restriction property if for all hulls L that are bounded away from the origin, conditional on the event $\{\gamma_{[0,\infty)} \cap L = \emptyset\}$, the distribution of $\gamma^*_{[0,\infty)}$ is the same as the distribution of the trace of a chordal SLE_κ process in $\mathbb{H}$, modulo a time re-parameterization. In words, suppose that SLE_κ has the restriction property. Then the distribution of all paths that are restricted not to hit L, and which are generated by SLE_κ in the half-plane, is the same as the distribution of all paths generated by SLE_κ in the domain $\mathbb{H} \setminus L$.

SLE has the restriction property for $\kappa = 8/3$ and for no other values of κ. A proof is given in [38] (a sketch of a proof appears in [29]), and in the same article it was also shown that

$$\mathbf{P}\big[\gamma_{[0,\infty)} \cap L = \emptyset\big] = |\Psi'(0)|^{5/8}. \tag{15.29}$$

Again, the restriction property can be translated into a similar property for arbitrary domains, and radial $\mathrm{SLE}_{8/3}$ also satisfies the restriction property. We refer to Lawler, Schramm and Werner [38] and Lawler [29] for more information.

15.4.4 Hausdorff Dimensions

Consider an SLE_κ process in the upper half-plane. If $\kappa \geq 8$ the trace of the process is space-filling, and therefore the Hausdorff dimension of the set $\gamma_{[0,\infty)}$ is 2. But for $\kappa \in (0,8)$ the Hausdorff dimension of $\gamma_{[0,\infty)}$ is a non-trivial number. Rohde and Schramm [44] showed that its value is bounded from above by $1+\kappa/8$, and the proof that for $\kappa \neq 4$ the Hausdorff dimension is in fact $1+\kappa/8$ was completed by Beffara [11, 10]. In the physics literature the Hausdorff dimensions of the curves that are believed to converge to SLE were predicted by Duplantier and Saleur [19, 45].

In the case $\kappa > 4$ the hull of SLE_κ is not a simple path, and it is natural to consider also the Hausdorff dimension of the boundary of K_t for some fixed value of $t > 0$. Its value is conjectured to be $1+2/\kappa$, because (based on a duality relation derived by Duplantier [19]) it is believed that the boundary of the hull for $\kappa > 4$ is described by $\mathrm{SLE}_{16/\kappa}$. The dimension of the hull boundary is known rigorously only for $\kappa = 6$ (where it is $4/3$) and for $\kappa = 8$ (where it is $5/4$). For $\kappa = 6$ this follows from the study of the "conformal restriction measures" in [38], for $\kappa = 8$ this is a consequence of the strong relation between loop-erased random walks and uniform spanning trees [36] (section 15.5.3).

15.5 SLE and Discrete Models

For a number of discrete lattice models, the scaling limit (of some of its observables) has been proven to be SLE. For many more models such a connection is only conjectured. Typically the stochastic measure of these models induces a measure on paths which in the scaling limit converges to the trace of an SLE process.

15.5.1 Critical Percolation

We define site percolation on the triangular lattice as follows. All vertices of the lattice are independently coloured blue with probability p or yellow with probability $1-p$. An equivalent, visually more attractive, viewpoint is to say that we colour all hexagons of the dual lattice blue or yellow with probabilities p and $1-p$, respectively. It is well-known that for $p \leq 1/2$, there is almost surely no infinite cluster of connected blue hexagons, while for $p > 1/2$ there a.s. exists a unique infinite blue

cluster. This makes $p = 1/2$ the critical point for site percolation on the triangular lattice. This critical percolation model is discussed here.

Let us for now restrict ourselves to the half-plane. Suppose that as our boundary conditions, we colour all hexagons intersecting the negative real line yellow, and all hexagons intersecting the positive real line blue. All other hexagons in the half-plane are independently coloured blue or yellow with equal probabilities. Then there exists a unique path over the edges of the hexagons, starting in the origin, which separates the cluster of blue hexagons attached to the positive real half-line from the cluster of yellow hexagons attached to the negative real half-line. This path is called the chordal exploration process from 0 to ∞ in the half-plane. It is the unique path from the origin such that at each step there is a blue hexagon on the right, and a yellow hexagon on the left. See Fig. 15.8 for an illustration.

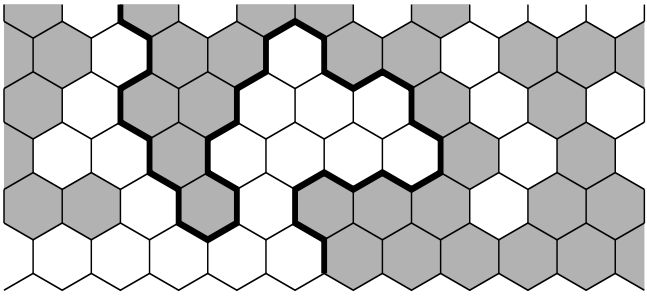

Fig. 15.8 Part of the percolation exploration process in the half-plane.

The exploration process depends only on the hexagons it passes. This makes it possible to generate it dynamically as follows. Initially, only the hexagons on the boundary receive a colour. Then after each step, the exploration process meets a hexagon, which may or may not have been coloured. If it has not yet been coloured, its colour is decided with equal probability for yellow or blue. Then the exploration process proceeds always keeping the yellow hexagon on its left. Note that the tip of the process cannot become trapped, because it is forced to reflect off into the open if it meets an already coloured hexagon. This property it has in common with the trace of a chordal SLE process. The process, here described for the half-plane, can be generalized without difficulty to other domains. In addition, it is easy to envision closed polygons to be generated by the percolation process. Each percolation configuration in a domain of which the entire boundary has one colour, induces closed polygons separating the blue from the yellow hexagons. The partition function of such polygons is a sum over all possible closed polygons on the infinite hexagonal lattice, with a weight 1/2 for each hexagon touching the polygon. If this polygon is interpreted as one of the domain walls in the percolation process, each hexagon touching the polygon has to be coloured with probability 1/2, all others being free. Besides the stochastics of the local exploration behaviour of such paths, which is

the same as that of the open path far from the boundary, this partition function also induces the distribution of the length of such paths.

Smirnov [51] proved that in the continuum limit, the exploration process is conformally invariant. Together with the results on SLE_6 developed by Lawler, Schramm and Werner, this should prove that the exploration process converges to the trace of SLE_6 in the half-plane. Thus, SLE_6 may be used to calculate properties of critical percolation. Some examples are described in section 15.6.

15.5.2 The Harmonic Explorer

The harmonic explorer is a random path similar to the exploration process of critical percolation. It was defined recently by Schramm and Sheffield as a discrete process that converges to SLE_4 [48]. To define the harmonic explorer, consider an approximation of a bounded domain with hexagons, as in Fig. 15.9. As we did for critical percolation, we partition the set of hexagons on the boundary of our domain into two components, and colour the one component yellow and the other blue. The hexagons in the interior are uncoloured initially.

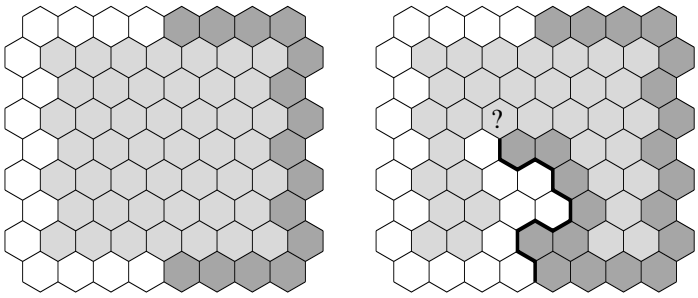

Fig. 15.9 Left: the initial configuration for the harmonic explorer, with blue hexagons (dark faces), yellow hexagons (white faces) and uncoloured hexagons (light faces). Right: a part of the harmonic explorer process. The colour of the marked hexagon is determined as described in the text.

The harmonic explorer is a path over the edges of the hexagons that starts out on the boundary with a blue hexagon on its right and a yellow hexagon on its left. It turns left when it meets a blue hexagon, and it turns right when it meets a yellow hexagon. The only difference with the exploration process of critical percolation is in the way the colour of an as yet uncoloured hexagon is determined. For the harmonic explorer this is done as follows.

Suppose that the harmonic explorer meets an uncoloured hexagon (see Fig. 15.9). Let f be the function, defined on the faces of the hexagons, that takes the value 1 on the blue hexagons, the value 0 on the yellow hexagons, and is discrete harmonic on the uncoloured hexagons (for each hexagon the value of f is the average of that of its neighbors). Then the probability that the hexagon whose colour we want to

determine is made blue, is given by the value of f on this hexagon. Proceeding in this way, we obtain a path crossing the domain between the two points on the boundary where the blue and yellow hexagons meet. In the scaling limit this path converges to the trace of chordal SLE_4.

15.5.3 Loop-Erased Random Walks and Uniform Spanning Trees

In this subsection we consider loop-erased random walks (LERW's) and uniform spanning trees (UST's). We shall define both models first, and we will point out the close relation between the two. Schramm [46] already proved that the LERW converges to SLE_2 under the assumption that the scaling limit exists and is conformally invariant. In the same work, he also conjectured the relation between UST's and SLE_8. The final proofs of these connections were given by Lawler, Schramm and Werner in [36]. Their proofs hold for general lattices, but for simplicity, we shall restrict our description here to finite subgraphs of the square grid $\delta\mathbb{Z}^2$ with mesh $\delta > 0$.

Suppose that G is a finite connected subgraph of $\delta\mathbb{Z}^2$. Let u be a vertex of G and let V be a collection of vertices of G not containing u. Then the LERW from u to V in G is defined by taking a simple random walk in G from u to V and erasing all its loops in chronological order. More precisely, if $\big(\omega(0),\ldots,\omega(T_V)\big)$ are the vertices visited by a simple random walk starting from u and stopped at the first time T_V when it visits a vertex in V, then its loop-erasure $\big(\beta(0),\ldots,\beta(T)\big)$ is defined as follows. We start by setting $\beta(0) = \omega(0)$. Then for $n \in \mathbb{N}$ we define inductively: if $\beta(n) \in V$ then $T = n$ and we are done, and otherwise we set $\beta(n+1) = \omega(1 + \max\{m \le T_V : \omega(m) = \beta(n)\})$. In words: the next step is taken to be the last exit from $\beta(n)$. The path $\big(\beta(0),\ldots,\beta(T)\big)$ is then a sample of the LERW in G from u to V.

A spanning tree T in G is a subgraph of G such that every two vertices of G are connected via a unique simple path in T. A *uniform* spanning tree (UST) in G is a spanning tree chosen with the uniform distribution from all spanning trees in G. There is an interesting connection between UST and LERW:

Theorem 7. *The unique path between two distinct vertices u and v on a UST, is distributed as the LERW from u to v.*

Proof. There are several ways to see this connection. One proceeds via a Monte Carlo (MC) process to generate UST. A MC process is a stochastic process of which the stationary distribution is the measure one wants to sample. The MC process used here is driven by a random walk on the graph G. Every time an edge is traversed by the random walk it is included in the tree, at the expense of the edge of the newly occupied node, by which the random walk left the node on its previous visit. Since that edge is the first step from that node to the current position in the random walk, the loop is removed. The edge added and the one removed need not be different. That the uniform measure is stationary under this process, follows from the fact that

for every move in the process there is precisely one counter move, and it is equally probable. Moreover, when the walk starts in a node u, the first time it arrives in a preselected subset V, the unique path from u to the arrival point in V is precisely a LERW.

An interesting collorary of this result is that the LERW is symmetric between beginning and end. This is not at all obvious from its definition. An algorithm to generate UST's, somewhat related to the MC process above is known as Wilson's algorithm [60].

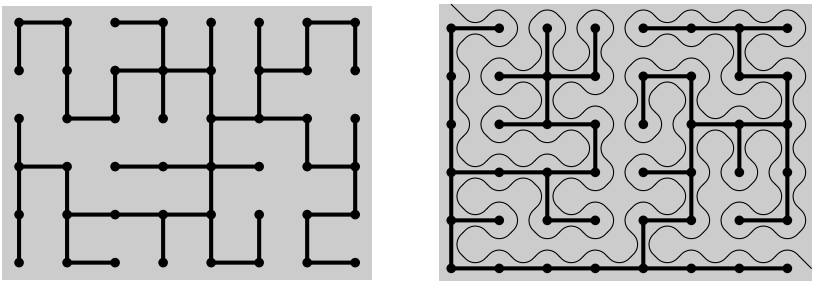

Fig. 15.10 Examples of spanning trees on a rectangular graph. In the right-hand panel, the nodes in the left and bottom boundary are fully connected. The thin curve from the lower right to the upper left corner closely surrounds the tree, and is space filling. Such paths are called Peano curves.

The connection between LERW and SLE_2 can be described as follows. Choose a subgraph of $\mathbb{Z}^2$, with a single, connected boundary, and a UST on it. Figure 15.10 in the left panel shows a rectangular example with the tree indicated by solid bonds. The unique path between a node u on the boundary and another node v has SLE_2 as its scaling limit. When v (or its limiting point in the scaling procedure) is also on the boundary in the chordal process, and if v is in the interior, it is radial SLE.

To see in what way UST converges to SLE_8, consider the right panel of Fig. 15.10. It also shows a rectangular subgraph of $\mathbb{Z}^2$ with a spanning tree. Now the left and bottom boundary nodes are fully connected to each other. One can trace a path which closely surrounds the spanning tree. For spanning trees on the square lattice these paths are called Peano curves. It visits all the sites of a square lattice with half the mesh size of the original lattice, while it never intersects itself. In general, non-intersecting paths visiting every site of a graph once are called Hamiltonian walks.

For this specific boundary condition on the spanning tree, such that all vertices on the left and bottom of the rectangle are connected, the tree induces a Peano curve which runs from the lower right corner to the upper left, and visits all sites in between. It is this path which has chordal SLE_8 as its scaling limit.

While we need open paths from the boundary to make the connection to SLE, the LERW and UST also define closed polygons of well-defined distributions as follows. Take a UST, and add one bond uniformly chosen from all edges not included in the tree. This creates a closed polygon, with the properties of the LERW.

The same distribution would be obtained by starting a LERW at some point in the lattice, and terminating it the first time it visits the starting point after it has been away from the starting point at least two steps. This last restriction is only to suppress trivial walks of two steps. A closed Peano curve can be defined by removing one bond from the spanning tree, which necessarily cuts it in two. The closed Peano curve surrounding each of the two parts is a closed polygon. These two polygons together fill the original domain. The same distribution of polygons can be obtained by adding an arbitrary bond to the tree, and taking the Peano curve which traces the inside of the loop uniquely created by the extra bond.

15.5.4 Self-Avoiding Walks

A self-avoiding walk (SAW) of length n on the square lattice $\delta\mathbb{Z}^2$ with mesh $\delta > 0$ is a nearest-neighbour path $\omega = \big(\omega(0), \omega(1), \ldots, \omega(n)\big)$ on the vertices of the lattice, such that no vertex is visited more than once. In this subsection we shall restrict ourselves to SAW's that start in the origin and stay in the upper half-plane afterwards. The idea is to define a stochastic process, called the half-plane infinite SAW, that in the scaling limit $\delta \downarrow 0$ is believed to converge to chordal $\mathrm{SLE}_{8/3}$.

Following [37] we write Λ_n^+ for the set of all SAW's ω of length n that start at the origin, and stay above the real line afterwards. For a given ω in Λ_n^+, let $Q_k^+(\omega)$ be the fraction of walks ω' in Λ_{n+k}^+ whose beginning is ω, i.e. such that $\omega'(i) = \omega(i)$ for $0 \le i \le n$. Define $Q^+(\omega)$ as the limit of $Q_k^+(\omega)$ as $k \to \infty$. Then $Q^+(\omega)$ is roughly the fraction of very long SAW's in the upper half-plane whose beginning is ω. It was shown by Lawler, Schramm and Werner that the limit $Q^+(\omega)$ exists [37].

Now we can define the *half-plane infinite self-avoiding walk* as the stochastic process X_i such that for all $\omega = \big(0, \omega(1), \ldots, \omega(n)\big) \in \Lambda_n^+$,

$$\mathbf{P}[X_0 = 0, X_1 = \omega(1), \ldots, X_n = \omega(n)] = Q^+(\omega). \tag{15.30}$$

We believe that the scaling limit of this process as the mesh δ tends to 0 exists and is conformally invariant. By the restriction property the scaling limit has to be $\mathrm{SLE}_{8/3}$, as pointed out in [37]. At this moment it is unknown how the existence, let alone the conformal invariance, of the scaling limit can be proved. However, the knowledge of its properties is still growing [57].

Lawler, Schramm and Werner [37] also explain how one can define a natural measure on SAW's with arbitrary starting points, leading to conjectures relating SAW's to chordal and radial $\mathrm{SLE}_{8/3}$ in bounded simply-connected domains. The article further discusses similar conjectures for self-avoiding polygons, and predictions for the critical exponents of SAW's that can be obtained from SLE. We shall not go into these topics here.

15.5.5 The Critical Ising Model

The Ising model is the prototypical model for a phase transition. It is solvable not only at the critical point, but also at other temperatures. In the physics literature the conformal invariance of its scaling is almost always taken for granted. As a consequence there were not many attempts by physicists to formally prove this property. However, the model is so extensively studied and so much is known about it in detail that it may well be that some assertions in the physics literature of the conformal invariance of certain correlation functions, are open to complete proof.

Only recently Smirnov [53] presented a formal proof that some observables in the scaling limit of the Ising model are conformally invariant, and as a consequence are $\mathrm{SLE}_{16/3}$. This proof is based on an exploration process of the Fortuin-Kasteleyn random cluster [23] representation of the model. This connection will be discussed in the next section, but the percolation exploration process, and that exploring the UST, discussed in the previous subsections 15.5.1 and 15.5.3 are examples of it. What Smirnov was able to prove is that the probability that a particular point z is on the trace of the exploration process, is the absolute value of a discrete analytic function of z. The phase of this function is proportional to the winding angle at which the trace passes z.

15.5.6 The Potts Model

So far in this section we discussed relations between SLE at specific values of κ to certain statistical lattice models. The results of SLE however suggest a further connection to continuous families of models. This subsection deals with the q-state Potts model, a natural generalization of the Ising model, which has $q = 2$. Below we will give a standard treatment [9], which relates the partition sum of the Potts model to an ensemble of multiple paths on the lattice. In the scaling limit these paths will be the candidates for the SLE processes.

The Potts model has on each site of a lattice a variable s_j which can take values in $\{1,2,\ldots,q\}$. Of these variables only nearest neighbours interact such that the energy is -1 if both variables are in the same state and 0 otherwise. The canonical partition sum is

$$Z = \sum_{\{s\}} \exp\left(\beta \sum_{\langle j,k\rangle} \delta_{s_j,s_k}\right). \tag{15.31}$$

The summation in the exponent is over all nearest-neighbour pairs of sites, and the external summation over all configurations of the s_j. The model is known to be disordered at high temperatures, and ordered at low temperatures. Here we are interested in the behaviour at the transition.

In order to make the connection with a path on the lattice, we express this partition sum in a high-temperature expansion, i.e. in powers of a parameter which is small when β is small. The first step is to write the summand as a product:

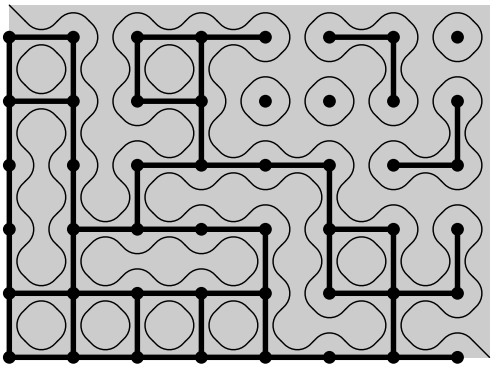

Fig. 15.11 Graph in the cluster expansion of the Potts model in a rectangular domain. The nodes of the left and bottom boundary are fully connected, so that there is one open path, from the top left to the bottom right corner.

$$Z = \sum_{\{s\}} \prod_{\langle j,k \rangle} \left[1 + (\mathrm{e}^{\beta} - 1)\delta_{s_j,s_k} \right]. \tag{15.32}$$

The product can be expanded in terms in which at every edge of the lattice a choice is made between the two terms 1 and $(\mathrm{e}^{\beta} - 1)\delta_{s_j,s_k}$. In a graphical notation we place a bond on every edge of the lattice where the second term is chosen, see Fig. 15.11. For each term in the expansion of the product the summation over the s-variables is trivial: if two sites are connected by bonds, their respective s-variables take the same value, and are independent otherwise. As a result the summation over $\{s\}$ results in a factor q for each connected component of the graph. Hence

$$Z = \sum_{\text{graphs}} (\mathrm{e}^{\beta} - 1)^b q^c, \tag{15.33}$$

where c is the number of connected components of the graph and b the number of bonds. This expansion is known by the name of Fortuin-Kasteleyn [23] cluster model. Note that, while q has been introduced as the (integer) number of states, in this expansion it can take any value.

It is convenient to rewrite the cluster expansion as an expansion of paths on a new lattice, called the surrounding lattice. The edges of the original lattice correspond to the vertices of the surrounding lattice. The clusters on the original lattice are rewritten into polygon decompositions of the new lattice. Every vertex of the surrounding lattice is separated into two non-intersecting path segments. These path segments intersect the corresponding edge of the original lattice if and only if this edge does not carry a bond of the graph, as follows:

As a result of these transformations the new lattice is decomposed into a collection of non-intersecting paths, as indicated in Fig. 15.11. Notice that every component of the original graph is surrounded by one of these closed paths, but also the closed circuits of the graph are inscribed by these paths. By Euler's relation the number of components c of the original graph can be expressed in the number of bonds b, the total number of sites N and the number of polygons p: $c = (N - b + p)/2$. An alternative expression for the partition sum is then

$$Z = \sum_{\text{graphs}} \left(\frac{e^{\beta} - 1}{\sqrt{q}} \right)^{b} q^{(N+p)/2}. \tag{15.34}$$

At the critical point β_c the relation $\exp(\beta_c) = 1 + \sqrt{q}$ holds, so that the partition sum simplifies.

We will now consider this model at the critical point on a rectangular domain. The lattice approximation of this domain is chosen such that the lower-left corner of the rectangle coincides with a site of the lattice, while the upper-right corner coincides with a site of the dual lattice. The sides of the rectangle are parallel to the edges of the lattice, as in Fig. 15.11. We choose as boundary condition that all edges that are contained in the left and lower sides of the rectangle carry bonds, and all edges that intersect the right and upper sides perpendicularly carry no bonds. For the spin variables this means that all the spins on the left and lower sides are in the same state, while all other spins are unconstrained.

In such an arrangement the diagrams in (15.34) include one path from the lower-right to the upper-left corner. All further paths are closed polygons, see Fig. 15.11. We take the scaling limit by covering the same domain with a finer and finer mesh. It is believed [44] that in the scaling limit the measure on the paths approaches that of chordal SLE_κ traces. From e.g. the Hausdorff dimension [10, 45] the relation between κ and q is

$$q = 2 + 2\cos(8\pi/\kappa) \tag{15.35}$$

where $4 \leq \kappa \leq 8$. Only in a few cases has this relationship between SLE_κ and the Potts partition sum been made rigorous. For instance, in the limit $q \to 0$, the graph expansion reduces to the uniform spanning tree, which has SLE_8 as its scaling limit.

15.5.7 The O(n) Model

We now turn to the O(n) model, which is another well-known model already discussed in Chapter 1, where a high-temperature expansion results in a sum over paths. Here the dynamic variables are n-component vectors of a fixed length, and the Hamiltonian is invariant under rotations in the n-dimensional space. The simplest high-temperature expansion is obtained when the Boltzmann weight is chosen as

$$\prod_{\langle j,k \rangle} (1 + x\, s_i \cdot s_j), \tag{15.36}$$

where the product is over nearest neighbours on a hexagonal lattice. The partition sum is obtained by integrating this expression over the directions of the spin vectors. As for the Potts model, one can expand the product and do the bookkeeping of the terms by means of graphs. In each factor in (15.36) the choice of the second term is indicated by a bond. Then the graphs that survive the integration over the spin variables have only even vertices, i.e. on the hexagonal lattice vertices with zero or two bonds. As a result the graphs consist of paths on the lattice. In a well-chosen normalization of the measure and the length of the spins, the partition sum is a sum over even graphs

$$Z = \sum_{\text{graphs}} x^L n^M, \tag{15.37}$$

where M is the number of closed loops, and L their combined length. Note that this expression for the partition sum is well-defined also when the number of spin components n is not integer. It is known [8, 41] that the critical point is at $x_c = [2 + (2-n)^{1/2}]^{-1/2}$ for $0 \le n \le 2$. When x is larger than this critical value, the model also shows critical behaviour.

Consider now this model on a bounded domain, and take a correlation function between two spins on the boundary. The diagrams that contribute to this function contain one path between the two specified boundary points and any number of closed polygons in the interior. We conjecture that at the critical value of x in the scaling limit, the measure on the paths between the two boundary spins approaches that of chordal SLE_κ for $n = -2\cos(4\pi/\kappa)$ and $8/3 \le \kappa \le 4$. For larger values of x, the scaling limit would again be SLE_κ, with the same relation between κ and n, but now with $4 \le \kappa \le 8$.

To conclude this section, we remark that the same partition sum (15.37) can also be viewed as the partition sum of a dilute Potts model on the triangular lattice, described in [43]. In this variant of the Potts model the spins take values in $\{0, 1, 2, \ldots, q\}$. The model is symmetric under permutations of the q positive values. The name dilute comes from the interpretation of the neutral value 0 as a vacant site. If neighbouring sites take different values, then one of them takes the value 0. The Boltzmann weight is a product over the elementary triangles of weights that depend on the three sites at the corners of the triangle. We take this weight to be 1 when all three sites are in the same state, vacant or otherwise. Triangles with one or two vacant sites have weights xy and x/y, respectively. The partition sum can be expanded in terms of domain walls between sites of different values. This expansion takes the form of (15.37) for $y^{12} = q = n^2$, which is the locus of the phase transition between an ordered phase and a disordered phase. Within this locus, the region with $x > x_c$ is a second-order transition. In the regime $x < x_c$ the transition is discontinuous, and the position $x = x_c$ separates the two regimes and is called the tricritical point. When $q = x = 1$ the site percolation problem on the triangular lattice is recovered, which is known to converge to SLE_6 in the scaling limit.

15.6 SLE Computations and Results

In this section we discuss some of the results that have been obtained from calculations involving SLE processes. Our aim in this section is not only to provide an overview of these results, but also to give an impression of the typical SLE computations involved, using techniques from stochastic calculus and conformal mapping theory.

This section is organized as follows: In the first subsection we discuss several SLE calculations independently from their connection with other models. The results we obtain will be key ingredients for further calculations. The second subsection gives a brief overview of how SLE can be applied to calculate the intersection exponents of Brownian motion. Finally, we will discuss results on critical percolation that have been obtained from its connection with SLE_6.

15.6.1 Several SLE Calculations

The purpose of this subsection is to show what kind of probabilities and corresponding exponents of events involving chordal SLE processes can be calculated. The results we find in this subsection are for whole ranges of κ, and might therefore have applications in various statistical models. In this overview we do not include proofs and extensive calculations. These can be found in [25] with references to the original literature.

15.6.1.1 Crossing and Passage Probabilities

Consider a chordal SLE_κ process inside the rectangle $\mathscr{R}_L := (0,L)\times(0,\pi)$, which goes from $\mathrm{i}\pi$ to L. If $\kappa > 4$ this process will at some random time τ hit the right edge $[L, L+\mathrm{i}\pi]$ of the rectangle, as in Fig. 15.12. Suppose that E denotes the event that up to this time τ, the SLE process has not hit the lower edge of the rectangle. Then the following holds:

Theorem 8. *The SLE_κ process as described above satisfies, for $\kappa > 4$,*

$$\boldsymbol{P}[E] \asymp \exp\left[-\left(1-\frac{4}{\kappa}\right)L\right] \quad \text{as } L\to\infty, \tag{15.38}$$

where $\asymp$ indicates that each side is bounded by some constant times the other side.

The theorem in this form is proved in [25]. Since the definition of chordal SLE in any domain is based on that in the upper half-plane, the first step in the proof is a mapping of the rectangle to $\mathbb{H}$.

The original form of the theorem is more general: Consider again an SLE_κ process crossing the rectangle $\mathscr{R}_L$ from $\mathrm{i}\pi$ to L. On the event E the trace γ has crossed

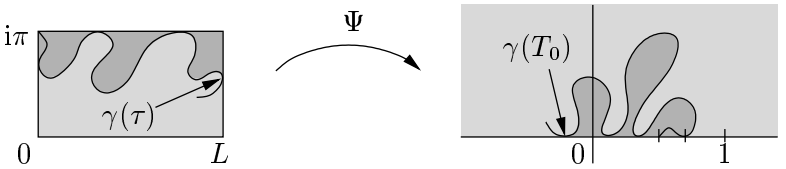

Fig. 15.12 An SLE process crossing a rectangle, and its translation to the upper half-plane. The darker grey areas represent the hulls of the processes.

the rectangle without hitting the bottom edge. So conditional on this event, the π-extremal distance between $[0,\mathrm{i}\pi]$ and $[L,L+\mathrm{i}\pi]$ in $\mathscr{R}_L \setminus K_\tau$ is well-defined. Let us call this π-extremal distance $\mathscr{L}$. Then one can prove the following generalization of theorem 8 [31].

Theorem 9. *For any $\lambda \geq 0$ and $\kappa > 4$,*

$$\boldsymbol{E}[1_E\, \mathrm{e}^{-\lambda \mathscr{L}}] \asymp \exp\big[-u(\kappa,\lambda)L\big] \qquad \text{as } L \to \infty, \tag{15.39}$$

where

$$u(\kappa,\lambda) = \lambda + \frac{\kappa - 4 + \sqrt{(\kappa-4)^2 + 16\kappa\lambda}}{2\kappa}. \tag{15.40}$$

The exponent $u(\kappa,\lambda)$ is called the one-sided crossing exponent, because it measures the extremal distance on one side of an SLE process crossing a rectangle. Observe that $u(\kappa,\lambda)$ reduces to the exponent $1-4/\kappa$ for $\lambda = 0$ as it should, because in this case theorem 9 is completely analogous to theorem 8.

There is an analogue of the one-sided crossing exponent for radial SLE, which we shall discuss only briefly here. The setup is as follows. We consider radial SLE_κ for any $\kappa > 0$, and set $A_t := \partial\mathbb{D} \setminus K_t$. Then the set A_t is either a piece of arc of the unit circle, or $A_t = \emptyset$. Let $r > 0$ and let $T(r)$ be the first time when the SLE process hits the circle $\{z : |z| = r\}$. Denote by E the event that $A_{T(r)}$ is non-empty. On the event E, let $\mathscr{L}$ be the π-extremal distance between the circles $\{z : |z| = 1\}$ and $\{z : |z| = r\}$ in $\mathbb{D} \setminus K_{T(r)}$, see Fig. 15.13.

Theorem 10. *For all $\lambda > 0$ and $\kappa > 0$,*

$$\boldsymbol{E}[1_E\, \mathrm{e}^{-\lambda \mathscr{L}}] \asymp r^{-\nu(\kappa,\lambda)} \qquad \text{as } r \downarrow 0, \tag{15.41}$$

where

$$\nu(\kappa,\lambda) = \frac{8\lambda + \kappa - 4 + \sqrt{(\kappa-4)^2 + 16\kappa\lambda}}{16}. \tag{15.42}$$

We call $\nu(\kappa,\lambda)$ the annulus crossing exponent of SLE_κ. A detailed proof of the theorem can be found in [32].

So far, we have considered several crossing events of SLE processes. A different kind of event, namely the event that the trace of SLE passes to the left of a given point z_0, was studied by Schramm in [47].

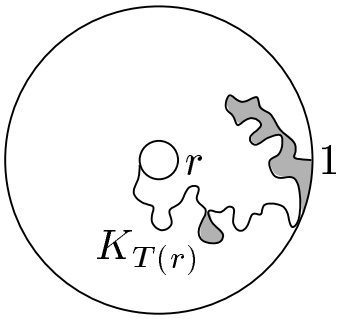

Fig. 15.13 An SLE process crossing an annulus.

Theorem 11. *Let $\kappa \in [0,8)$ and $z_0 = x_0 + \mathrm{i}y_0 \in \mathbb{H}$. Suppose that E is the event that the trace γ of chordal SLE$_\kappa$ passes to the left of z_0. Then*

$$\boldsymbol{P}[E] = \frac{1}{2} + \frac{\Gamma\left(\frac{4}{\kappa}\right)}{\sqrt{\pi}\,\Gamma\left(\frac{8-\kappa}{2\kappa}\right)}\, {}_2F_1\left(\frac{1}{2}, \frac{4}{\kappa}; \frac{3}{2}; -\frac{x_0^2}{y_0^2}\right) \frac{x_0}{y_0}. \tag{15.43}$$

This expression played an interesting role in the proof by Smirnov [51] that the percolation exploration process has SLE$_6$ as its scaling limit. When the half plane is mapped onto a unilateral triangle with the origin, ∞ and another real point mapped to corners of the triangle, the hypergeometric function appearing in the theorem for $\kappa = 6$ simplifies to a simple linear function. This suggested that things might become simpler for this value of κ and for a lattice model with hexagonal symmetry, in the case of site percolation on the triangular lattice.

15.6.2 Intersection Exponents of Planar Brownian Motion

One of the first successes of SLE was the determination of the intersection exponents of planar Brownian motion. One way of defining these exponents is as follows (see reference [30], which also presents alternative definitions). Let $k \geq 2$ and $p_1, \ldots, p_k$ be positive integers. At time $t = 0$, from each of the points $(0, j)$ (for $j \in \{1, \ldots, k\}$) we start p_j planar Brownian motions. Then we can define an exponent $\xi(p_1, \ldots, p_k)$ from the probability that at time t none of the Brownian walkers has hit the path of another one that started at a different initial position. Formally, denote by $\mathscr{B}_t^j$ the union of the traces of the p_j Brownian motions started from (O, j) up to time t. Then

$$\mathbf{P}\left[\forall i \neq j \in \{1, \ldots, k\}, \mathscr{B}_t^i \cap \mathscr{B}_t^j = \emptyset\right] \asymp \left(\sqrt{t}\right)^{-\xi(p_1, \ldots, p_k)} \tag{15.44}$$

when $t \to \infty$. The exponent $\xi(p_1,\ldots,p_k)$ is called the intersection exponent between k packets of $p_1,\ldots,p_k$ Brownian motions.

If we further require that the Brownian motions stay in the upper half-plane, we get different exponents $\tilde{\xi}(p_1,\ldots,p_k)$ defined by

$$\mathbf{P}\big[\forall i \neq j \in \{1,\ldots,k\}, \mathscr{B}_t^i \cap \mathscr{B}_t^j = \emptyset \text{ and } \mathscr{B}_t^i \subset \mathbb{H}\big] \asymp \big(\sqrt{t}\big)^{-\tilde{\xi}(p_1,\ldots,p_k)} \tag{15.45}$$

when $t \to \infty$. We could also *condition* on the event that the Brownian motions stay in the upper half-plane. The corresponding exponents are $\hat{\xi}(p_1,\ldots,p_k)$. They are related to the previous half-plane exponents by

$$\hat{\xi}(p_1,\ldots,p_k) = \tilde{\xi}(p_1,\ldots,p_k) - (p_1 + \ldots + p_k), \tag{15.46}$$

since the probability that a Brownian motion started in the half-plane stays in the half-plane up to time t decays like $t^{-1/2}$.

Duplantier and Kwon [20] predicted the values of the intersection exponents $\xi(p_1,\ldots,p_k)$ and $\hat{\xi}(p_1,\ldots,p_k)$ in the case where all p_i are equal to 1. In the series of papers [31, 32, 33, 34], Lawler, Schramm and Werner confirmed these predictions rigorously, and generalized them. Here, we will give an impression of the arguments used in the first paper [31], and then we will summarize the main conclusions of the series.

15.6.2.1 Intersection Exponents Generalized

In [30] Lawler and Werner show how the definition of the Brownian intersection exponents can be extended in a natural way. This leads to the definition of the exponents $\tilde{\xi}(\lambda_1,\ldots,\lambda_k)$ for all $k \geq 1$ and all non-negative real numbers $\lambda_1,\ldots,\lambda_k$, and of the exponents $\xi(\lambda_1,\ldots,\lambda_k)$ for all $k \geq 2$ and nonnegative real numbers $\lambda_1,\ldots,\lambda_k$, at least two of which must be at least 1.

It is then convenient to define the exponents not in terms of ordinary Brownian motions, but of Brownian excursions [30, 31]. A Brownian excursion in a domain is a measure of Brownian motions up to the time they hit the boundary, in the limit that the starting point is taken to the boundary, with an appropriate normalization for the measure to remain bounded and non-zero. Let $\mathscr{R}_L$ be the rectangle $(0,L) \times (0,\pi)$, and denote by ω the path of a Brownian excursion in $\mathscr{R}_L$ started from the left side. Let A be the event that the Brownian excursion crosses the rectangle from the left to the right. In other words that the right boundary is hit before the bottom or top boundary is hit. On this event, let D_+ and D_- be the domains remaining above and below ω in $\mathscr{R}_L \setminus \omega$, respectively, and let $\mathscr{L}_+$ and $\mathscr{L}_-$ be the π-extremal distances between the left and right edges of the rectangle in these domains. We refer to Fig. 15.14 for an illustration.

By symmetry, the distributions of $\mathscr{L}_+$ and $\mathscr{L}_-$ are the same. The exponent $\tilde{\xi}(1,\lambda)$ is characterized by

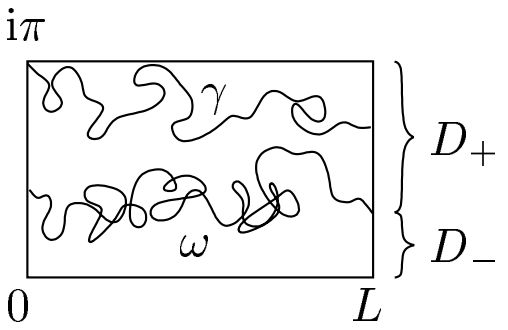

Fig. 15.14 An SLE_6 trace γ and a Brownian excursion ω crossing a rectangle.

$$\mathbf{E}_B[1_A\, \mathrm{e}^{-\lambda \mathscr{L}_+}] = \mathbf{E}_B[1_A\, \mathrm{e}^{-\lambda \mathscr{L}_-}] \asymp \mathrm{e}^{-\tilde{\xi}(1,\lambda)L} \qquad \text{as } L \to \infty \tag{15.47}$$

where $\mathbf{E}_B$ is used to indicate expectation with respect to the Brownian excursion measure. Likewise, $\tilde{\xi}(\lambda_+, 1, \lambda_-)$ is characterized by

$$\mathbf{E}_B[1_A\, \mathrm{e}^{-\lambda_+ \mathscr{L}_+} \mathrm{e}^{-\lambda_- \mathscr{L}_-}] \asymp \mathrm{e}^{-\tilde{\xi}(\lambda_+,1,\lambda_-)L} \qquad \text{as } L \to \infty. \tag{15.48}$$

It is quite remarkable that the weighting of the crossing event with the π-extremal distance has the same effect as the conditioning on not hitting the path of another Brownian excursion.

Another major result from [30] is the theorem below, which gives the so-called cascade relations between the Brownian intersection exponents. Together with an analysis of the asymptotic behaviour of the exponents (theorems 11 and 12 in [30]), these relations show that it is sufficient to determine the exponents $\xi(1,1,\lambda)$, $\tilde{\xi}(1,\lambda)$ and $\tilde{\xi}(\lambda,1,\lambda)$ for $\lambda \geq 0$ to know all the intersection exponents.

Theorem 12. *The exponents $\tilde{\xi}(\lambda_1,\ldots,\lambda_k)$ and $\xi(\lambda_1,\ldots,\lambda_k)$ are invariant under permutations of their arguments. Moreover, they satisfy the following cascade relations:*

$$\tilde{\xi}(\lambda_1,\ldots,\lambda_k) = \tilde{\xi}\big(\lambda_1,\ldots,\lambda_{j-1},\tilde{\xi}(\lambda_j,\ldots,\lambda_k)\big); \tag{15.49}$$

$$\xi(\lambda_1,\ldots,\lambda_k) = \xi\big(\lambda_1,\ldots,\lambda_{j-1},\tilde{\xi}(\lambda_j,\ldots,\lambda_k)\big). \tag{15.50}$$

These relations not only determine all of the $\tilde{\xi}$ in terms of a few, they also give a restriction on what form these can take. The final expressions can be computed by making use of SLE. Since the argument is relatively short, we give it here.

15.6.2.2 An Example Calculation

Suppose that we start an SLE_6 process from $\mathrm{i}\pi$ to L to the same rectangle $\mathscr{R}_L$ in which the Brownian excursion ω is already defined. In what follows, it is crucial that this process, as well as the Brownian excursion, have the locality property. In our present setup, this implies that as long as the SLE_6 trace does not hit ω, it doesn't matter whether we regard it as an SLE_6 in the domain $\mathscr{R}_L$ or in the domain D_+. Since SLE_κ has this property only for $\kappa = 6$, the following argument works only for this special value of κ.

Let us denote by γ the trace of the SLE_6 process up to the first time that it hits $[L, L+\mathrm{i}\pi]$, and let E be the event that γ is disjoint from ω and that ω crosses the rectangle from left to right. See Fig. 15.14. On the event E, the π-extremal distance between $[0,\mathrm{i}\pi]$ and $[L, L+\mathrm{i}\pi]$ in the domain between γ and ω is well-defined. We call this π-extremal distance $\mathscr{L}$. To obtain the value of $\tilde{\xi}(1,\lambda)$, our strategy is to express the asymptotic behaviour of $f(L) = \mathbf{E}[1_E \exp(-\lambda\mathscr{L})]$ in two different ways.

On the one hand, when ω is given, $1_E \exp(-\lambda\mathscr{L})$ is comparable to $\exp[-u(6,\lambda)\mathscr{L}_+]$ by theorem 9. We therefore get

$$f(L) \asymp \mathbf{E}_B[1_A \, \mathrm{e}^{-u(6,\lambda)\mathscr{L}_+}] \asymp \mathrm{e}^{-\tilde{\xi}(1,u(6,\lambda))L}. \tag{15.51}$$

On the other hand, when γ is given, the distributions of $\mathscr{L}$ and $\mathscr{L}_-$ are the same by the conformal invariance of the Brownian excursion. But also, given $\mathscr{L}_+$, the probability of the event E is comparable to $\exp(-\mathscr{L}_+/3)$ by theorem 8. Therefore

$$f(L) \asymp \mathbf{E}_B[1_A \, \mathrm{e}^{-\mathscr{L}_+/3} \mathrm{e}^{-\lambda\mathscr{L}_-}] \asymp \mathrm{e}^{-\tilde{\xi}(1/3,1,\lambda)L}. \tag{15.52}$$

By the cascade relations, $\tilde{\xi}(1/3,1,\lambda) = \tilde{\xi}\big(1,\tilde{\xi}(1/3,\lambda)\big)$. Hence, comparing the two results we obtain

$$\tilde{\xi}(1/3,\lambda) = u(6,\lambda) = \frac{6\lambda + 1 + \sqrt{1+24\lambda}}{6} \tag{15.53}$$

since $\tilde{\xi}(1,\lambda)$ is strictly increasing in λ. Finally, this result gives us for example $\tilde{\xi}(1,\lambda)$, because $\tilde{\xi}(1/3,1/3) = 1$, and then the cascade relations give

$$\tilde{\xi}(1,\lambda) = \tilde{\xi}\big(\tilde{\xi}(1/3,1/3),\lambda\big) = \tilde{\xi}\big(1/3,\tilde{\xi}(1/3,\lambda)\big). \tag{15.54}$$

15.6.2.3 Summary of Results

As we mentioned before, the series of papers by Lawler, Schramm and Werner [31, 32, 33, 34] led to the determination of all Brownian intersection exponents we defined above. We state their conclusions in a few equations.

For all integers $k \geq 2$ and all $\lambda_1, \ldots, \lambda_k \geq 0$,

$$\tilde{\xi}(\lambda_1,\ldots,\lambda_k) = \frac{1}{24}\left[1+\sum_{j=1}^{k}\left(\sqrt{1+24\lambda_j}-1\right)\right]^2 - \frac{1}{24} \tag{15.55}$$

For all integers $k \geq 2$ and all $\lambda_1,\ldots,\lambda_k \geq 0$, at least two of which are at least 1,

$$\xi(\lambda_1,\ldots,\lambda_k) = \frac{1}{48}\left[\sum_{j=1}^{k}\left(\sqrt{1+24\lambda_j}-1\right)\right]^2 - \frac{1}{12} \tag{15.56}$$

For $k=2$ the requirement that at least two of the λ be ≥ 1, may be replaced by $\lambda_1 > 1$ and $\lambda_1 \in \mathbb{Z}$ and $\lambda_2 \geq 0$.

To the physicist these exponents, based on π-extremal distance, may seem artificial, but for integer λ they are still the intersection exponents of packets of Brownian motions. It is worth noting also that those exponents need not be rational.

From earlier work of Lawler [26, 27, 28], it is known that some of these exponents are related to the Hausdorff dimensions of special subsets of the Brownian paths. Indeed, suppose that we denote by $B[0,1]$ the trace of a planar Brownian motion up to time 1. Then the Hausdorff dimension of its frontier (the boundary of the unbounded connected component of $\mathbb{C}\setminus B[0,1]$), is $2-\xi(2,0) = 4/3$. The Hausdorff dimension of the set of cut points (those points z such that $B[0,1]\setminus\{z\}$ is disconnected) is $2-\xi(1,1) = 3/4$. Finally, the set of pioneer points of $B[0,1]$ (those points z such that for some $t\in[0,1]$, $z = B_t$ is in the frontier of $B[0,t]$) has Hausdorff dimension $2-\xi(1,0) = 7/4$. Not only do these exponents figure in the percolation problem, they are precisely the Hausdorff dimension of the same subsets of the percolation exploration process, i.e. the frontier, the cut points and the pioneer points. This shows how closely the random walk and critical percolation are related.

15.6.3 Results on Critical Percolation

The connection between SLE_6 and critical site percolation on the triangular lattice can be used to verify rigorously the values of certain percolation exponents. In this subsection we review how for example the multi-arm exponents for percolation can be calculated from the one-sided crossing exponent and the annulus crossing exponent of SLE_6. Predictions of the values of these exponents have appeared in several places in the physics literature, see e.g. [18] and references therein.

15.6.3.1 Half-Plane Exponents

Consider critical site percolation on the triangular lattice with fixed mesh. Let $A^+(r,R)$ be the semi-annulus $\{z : r < |z| < R, \mathrm{Im}\, z > 0\}$, and denote by $f_k^+(r,R)$ the probability that there exist k disjoint crossings of arbitrary colours from the inner circle to the outer circle in $A^+(r,R)$. By a crossing we mean a sequence of distinct connected

hexagons, all in the same colour, whose first and last hexagons are adjacent to a hexagon intersecting the inner and outer circle, respectively. Obviously, r has to be large enough if the definition of $f_k^+(r,R)$ is to make sense, i.e. $r > \text{const}(k)$.

The probability $f_k^+(r,R)$ does not depend on the choice of colours of the different crossings. The reason for this is that one can always flip the colours of crossings without changing probabilities. This needs to be done with some care, because flippings conditioned on certain events may change the probability of the configuration. One can start by considering the right-most crossing. If desired, its colour can be decided by flipping the colours of all hexagons. Then one proceeds by each time considering the right-most crossing to the left of the previous one. If desired, its colour can be changed by flipping the colours of all hexagons to the left of this previous crossing. In the end one obtains a configuration with all crossings in the desired colours, without having changed probabilities. In particular, we can take $f_k^+(r,R)$ to be the probability of k crossings of alternating colours.

To make the connection with SLE, suppose that we colour all hexagons that intersect the boundary of the semi-annulus blue if they are on the counter-clockwise part of the boundary from $-r$ to R, and yellow if they are on the clockwise boundary from $-r$ to R. Then the probability $f_k^+(r,R)$ is exactly the probability that the exploration process from $-r$ to R makes k crossings before it hits the interval $[r,R]$. By Smirnov's result, this translates in the scaling limit into the probability that a chordal SLE_6 process from $-r$ to R in the semi-annulus makes k crossings before it hits the interval $[r,R]$, see Fig. 15.15.

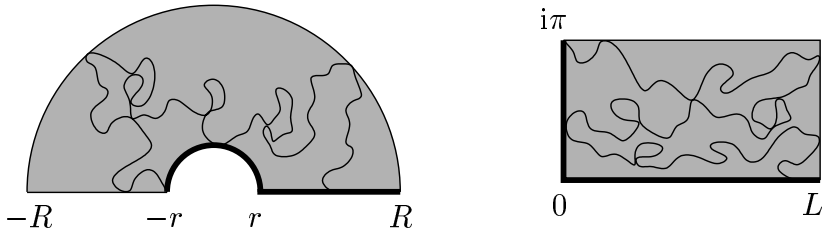

Fig. 15.15 An SLE_6 process which crosses a semi-annulus three times, and the equivalent process in a rectangle. The thick part of the boundary is the part coloured blue.

It is more convenient now to map the problem to a rectangle using the logarithmic map. Suppose that $g_k^+(L)$ denotes the probability that an SLE_6 trace from $\mathrm{i}\pi$ to L in the rectangle $\mathscr{R}_L := (0,L) \times (0,\pi)$ makes k horizontal crossings before it hits the bottom. Then, by conformal invariance, we want to determine $g_k^+(L)$ for $L = \log(R/r)$. For $k = 1$ theorem 8 immediately gives $g_1^+(L) \asymp \exp(-L/3)$. Exponents for larger k can be determined using theorem 9. This is a good example of the use of that theorem.

Let T be the time at which the SLE_6 process has crossed the rectangle for the first time, and let E be the event that up to time T the process has not hit the bottom. Then the process still has to make $k-1$ crossings in the domain below this first

crossing. Hence, if $\mathscr{L}$ denotes the π-extremal distance between the left and right edges in this remaining domain, we have

$$g_k^+(L) = \mathbf{E}[1_E\, g_{k-1}^+(\mathscr{L})]. \tag{15.57}$$

When we define $g_k^+(L) \asymp \exp(-v_k^+ L)$ we find $v_1^+ = 1/3$ from Theorem 8 and $v_k^+ = k(k+1)/6$ by applying recursively Theorem 9. For discrete percolation in the semi-annulus, this implies that

$$f_k^+(r,R) \asymp R^{-k(k+1)/6} \qquad \text{when } R \to \infty. \tag{15.58}$$

To make this transition to discrete percolation completely rigorous some more work is required. We refer to [52] for more details.

15.6.3.2 Plane Exponents

In order to obtain exponents for a point interior in a domain rather than at its boundary, we must use a radial process. Suppose that $A(r,R)$ is an approximation of the full annulus $\{z : r < |z| < R\}$ by hexagons, where r is again assumed to be large enough. We can define an exploration process in this annulus as follows. We colour all hexagons intersecting the inner circle blue. The exploration process starts at R with a blue hexagon on its right (above it), and a yellow hexagon on its left. Each time the exploration process hits a hexagon on the outer circle that was not visited before, we look at the phase angle of the position of the tip of the trajectory at that time (defining this phase to be continuous in time). If the phase is positive, the hexagon on the boundary is coloured blue, and otherwise it is coloured yellow.

When the exploration process described above first hits the inner circle, it defines unambiguously a clockwise-most blue crossing of the annulus and a counter-clockwise-most yellow crossing, such that the point R lies between them. Moreover, it can be easily seen that afterwards, the exploration process continues like a chordal process in the remaining domain between these two crossings, where the outer circle may now be assumed to be coloured yellow. This remaining domain is equivalent to a semi-annulus. Therefore, the probability that the process crosses this remaining domain $k-2$ times before it disconnects the inner circle from the outer circle is equal to the probability that there are $k-2$ crossings of arbitrary colours of this domain, as we discussed in the previous subsection.

Let $f_k(r,R)$ be the probability that the exploration process crosses the annulus a total number of $k-1$ times. Then for even k, $f_k(r,R)$ is just the probability that there exist k crossing paths of the annulus, which are not all of the same colour. (To avoid confusion one must carefully distinguish the crossings by the exploration process, and the existence of crossing paths on the percolation clusters.) In this case we have the freedom of choosing alternating colours for the crossing paths, and then the point R is always between a right-most blue and a left-most yellow crossing, which proves the point. For odd k, the situation is different, and $f_k(r,R)$ is not equal to the probability that there exist k crossings of the annulus which are not all of the

same colour. However, it can be shown that the two probabilities differ only by a multiplicative constant, see [52].

We now make the connection with SLE_6. In the continuum limit, the discrete exploration process converges to the following SLE process. First, we do radial SLE_6 in the annulus from R to 0, up to the first time T that the process hits the inner circle. Afterwards, the process continues like a chordal SLE_6 process in the remaining domain. We further define E to be the event that up to time T, the process has not disconnected the inner circle from the outer circle. On this event, we let $\mathscr{L}$ denote the π-extremal distance between the two circles in the remaining domain.

Denote by $g_k(r,R)$ the probability that this SLE_6 process crosses the annulus $k-1$ times before it disconnects the inner circle from the outer circle. Then

$$g_k(r,R) = \mathbf{E}[1_E\, g^+_{k-2}(\mathscr{L})] \asymp \mathbf{E}[1_E\, \mathrm{e}^{-\nu^+_{k-2}\mathscr{L}}] \tag{15.59}$$

where $g^+_k(L)$ is the probability of k crossings of the rectangle $(0,L)\times(0,\pi)$, as before. Theorem 10 now tells us that $g_k(r,R) \asymp (R/r)^{-\nu_k}$, where

$$\nu_k = \nu(6,\nu^+_{k-2}) = \frac{k^2-1}{12}. \tag{15.60}$$

Returning to discrete percolation, it follows from this result that the probability of k crossings of the annulus $A(r,R)$ which are not all of the same colour behaves like

$$f_k(r,R) \asymp R^{-(k^2-1)/12} \qquad \text{when } R\to\infty. \tag{15.61}$$

Again, all of this has been made rigorous [52]. Observe also that we can again interpret the result in terms of crossings of clusters. In this case we have that for k even, $f_k(r,R)$ is comparable to the probability that there exist $j=k/2$ disjoint blue clusters crossing the annulus.

So far we have considered only the dichromatic exponents associated with the probability of k percolation crossings of an annulus that are *not* all of the same colour. The corresponding monochromatic exponents for k crossings that *are* of the same colour are known to have different values. They are not so easily accessible through SLE as the dichromatic exponents. However, SLE computations [35] have confirmed that the one-arm exponent ($k=1$) has the value $5/48$, and in the same article, a description of the backbone exponent ($k=2$) as the leading eigenvalue of a differential operator was given.

15.7 Discussion

While Schramm originally introduced SLE as the only possible candidate for the scaling limit of the loop-erased random [46] walk, the definition and properties of SLE were sufficiently general to allow Schramm to conjecture that SLE also describes the scaling limits of uniform spanning trees and critical percolation. Subse-

quently it was proved to be the scaling limit of several other models. In fact, it is believed that conformal invariance and stationarity is sufficient for a whole range of critical models to converge to SLE (section 15.5).

For this approach to be applicable to a lattice statistical model with local interaction (on a domain with a boundary), it must at least have the following properties.

(i) It must have a conformally invariant scaling limit.
(ii) SLE being a measure of curves, the model must induce a measure of non-crossing paths in the lattice.
(iii) Since the law for $\gamma_{t'} - g_t(\gamma_t)$ is the same as that for $g_t(\gamma_{t+t'})$ the image under g_t of $\gamma_{[0,t]}$ may have no other properties than the simple original boundary.
(iv) And because there is no drift in the driving term, there should be symmetry between the two sides of the curve.

The first condition is believed to be true for almost all models at an isotropic phase transition. But only in very rare cases has this been proved. Note in the second condition the difference between crossing and intersecting. This condition is easily satisfied, as one can take as paths the domain walls, between different values, of the variable. In a continuous model, level lines may figure as paths. In many cases where a diagrammatic expansion of the partition sum is possible, it may induce paths on the lattice. The third requirement, however, is rather restrictive. Together with (iv) it is known as the stationarity property. Consider as an example a model with a discrete variable on the lattice, taking four values. Without loss of generality, it can be described by two coupled Ising variables, σ_1 and σ_2. The curves we consider first are the domain walls of σ_1, which will be defined in such a way that they cannot cross. We must now choose boundary conditions compatible with this definition of the path, i.e. *in accordance with the condition on either side of these domain walls*. Clearly σ_1 must be fixed at ± 1 on the positive and negative real axis respectively. Now there are several choices to make. We may choose σ_2 to be fixed as well, on the boundary and on either side of the domain wall of σ_1. If σ_2 is the same on the positive and negative real axis, then this implies that the domain walls of σ_1 and those of σ_2 are not permitted to cross each other. If we choose σ_2 to be opposite on the positive and negative real axes, and consequently on either side of the path, the model must have domain walls for both Ising components, which cannot split up in separate domain walls. A third possibility is to choose σ_2 to be free on the boundary. This implies that it is also free on the domain wall of σ_1. However, after the path is mapped onto the real axis, the same point of the path has two images, far apart. It does not seem acceptable that σ_2 has strong correlations between these two points, as a result of their common history. The only way to avoid such correlations is to forbid all interactions between σ_2 variables accross a domain wall of σ_1. Finally, instead of a domain wall for σ_1, we may consider the curves separating one of the four states from the three others. Such domain walls have an intrinsic asymmetry, because on one side three states are allowed and on the other only one. Nonetheless, by special properties of the model this asymmetry may be lifted.

In summary we can say about models with multiple degrees of freedom, that it may be possible for SLE to describe their scaling limit, but the model must have a

number of very restrictive properties. It may be noted that the four-state Potts model, which is expected to be SLE_4, does indeed satisfy these restrictions. If it is written in terms of two Ising spins, the one does not interact accross the domain wall of the other. Furthermore the domain wall separating one state from the three others is probably symmetric as a result of the dual symmetry between the ordered and disordered phases.

Apart from being the candidate for the scaling limit of critical models, SLE also gives us an idea of how the convergence can be proved. One could try to describe the discrete path of the critical model by a Löwner evolution, and then prove that the driving function converges to Brownian motion. Indeed, this is the way in which the convergence of loop-erased random walks to SLE_2, and of the Peano curve winding around the uniform spanning tree to SLE_8 were proved. Recently, the harmonic explorer was added to the list, and it seems reasonable to believe that in the future more connections between discrete models and SLE will be established.

However, a limitation of SLE appears to be that it is only capable of describing a very specific aspect of the discrete models. In the Fortuin-Kasteleyn cluster formulation of the Potts model, for example, SLE describes the boundary of one special cluster connected to the boundary, as explained in section 15.5.6. An interesting question is then what can SLE tell us about the full configuration of clusters, rather than only about the boundary of one? Methods to describe this have been developed recently, starting with SLE_6 [12], and later for general SLE_κ [12, 58, 50, 13, 49, 59].

Interesting developments have taken place regarding the connection between SLE and conformal field theory, a subject not considered in this article. Various aspects of this connection have been studied in a series of papers by Michel Bauer and Denis Bernard [2, 3, 4, 5], showing for example how results from SLE can be computed in the CFT language. Another connection was proposed by John Cardy [15] who introduced a multiple SLE process. This he could connect with Dyson's Brownian process, and through it to the distribution of eigenvalues of ensembles of random matrices. Using the conformal restriction properties studied in [38], the work of Roland Friedrich and Wendelin Werner [21, 22, 55] further clarifies the link between the discrete systems and conformal field theory. Thus SLE may prove to be very useful in putting the ideas of conformal field theory on a mathematically more rigorous footing. Clearly an obvious open question is the proof that the q-state Potts model for all q, and the O(n) model for all n has SLE as scaling limit. It is conceivable that the approach by Smirnov [53], successful for the Ising model, is open to generalization. Unlike the case of percolation it is not based on a property in which the Ising model is qualitatively different from the other Potts models.

SLE is a promising field of research, and the literature on SLE is already quite vast and still growing. In this discussion we only touched upon some of the developments that have taken place, without the intention of providing a complete list. In conclusion, SLE seems invaluable for adding mathematical rigour to our understanding of the scaling limits of critical two-dimensional systems and their conformal invariance. This same fact makes SLE a mathematically and technically challenging object of study.

References

1. L. V. Ahlfors. *Conformal invariants: topics in geometric function theory*. McGraw-Hill, New York, 1973.
2. M. Bauer and D. Bernard. SLE_κ growth processes and conformal field theories. *Phys. Lett. B* 543:135–138, 2002. arXiv: math-ph/0206028.
3. M. Bauer and D. Bernard. Conformal Field Theories of Stochastic Loewner Evolutions. *Comm. Math. Phys.* 239:493–521, 2003. arXiv: hep-th/0210015.
4. M. Bauer and D. Bernard. SLE martingales and the Virasoro algebra. *Phys. Lett. B* 557:309–316, 2003. arXiv: hep-th/0301064.
5. M. Bauer and D. Bernard. Conformal transformations and the SLE partition function martingale. *Ann. Henri Poincaré* 5:289–326. arXiv: math-ph/0305061.
6. M. Bauer, D. Bernard, J. Houdayer. Dipolar SLE's. *J. Stat. Mech*. 0503:P001, 2005. arXiv:math-ph/0411038.
7. R. J. Baxter. *Exactly solved models in statistical mechanics*. Academic Press, London, 1982.
8. R. J. Baxter. q colourings of the triangular lattice. *J. Phys. A* 19:2821–2839, 1986.
9. R. J. Baxter, S. B. Kelland, and F. Y. Wu. Equivalence of the Potts model or Whitney polynomial with an ice-type model. *J. Phys. A* 9:397–406, 1976.
10. V. Beffara. The dimension of the SLE curves. *Ann. Prob.* 36:1421–1452, 2002. arXiv: math.PR/0211322.
11. V. Beffara. Hausdorff dimensions for SLE_6. *Ann. Prob.* 32:2606–2629, 2002. arXiv: math.PR/0204208.
12. F. Camia and C. M. Newman. Continuum nonsimple loops and 2D critical percolation. *J. Stat. Phys.* 37:157–173, 2004. arXiv: math.PR/0308122.
13. F. Camia, C. M. Newman. SLE(6) and CLE(6) from Critical Percolation. arXiv:math/0611116.
14. J. Cardy. Conformal invariance. In C. Domb and J. L. Lebowitz, editors, *Phase transitions and critical phenomena*, volume 11, pages 55–126. Academic Press, London, 1987.
15. J. Cardy. Stochastic Loewner Evolution and Dyson's Circular Ensembles. *J. Phys. A* 36:L379–L408, 2003. arXiv: math-ph/0301039.
16. J. Cardy. SLE for theoretical physicists. *Ann. Phys.* 318:81–118, 2005.
17. E. Domany, D. Mukamel, B. Nienhuis and A. Schwimmer. Duality relations and equivalences for models with O(n) and cubic symmetry. *Nucl. Phys.* B190:279, 1981.
18. B. Duplantier. Harmonic measure exponents for two-dimensional percolation. *Phys. Rev. Lett.* 82:3940–3943, 1999.
19. B. Duplantier. Conformally invariant fractals and potential theory. *Phys. Rev. Lett.* 84:1363–1367, 2000.
20. B. Duplantier and K-H. Kwon. Conformal invariance and intersections of random walks. *Phys. Rev. Lett.* 61:2514–2517, 1988.
21. R. Friedrich and W. Werner. Conformal fields, restriction properties, degenerate representations and SLE. *C. R. Acad. Sci. Paris Ser. I* 335:947–952, 2002. arXiv: math.PR/0209382.
22. R. Friedrich and W. Werner. Conformal restriction, highest-weight representations and SLE. *Comm. Math. Phys.* 243:105–122, 2003. arXiv: math-ph/0301018.
23. C. M. Fortuin and P. W. Kasteleyn. On the random cluster model 1: Introduction and relation to other models. *Physica* 57:536–564, 1972.
24. W. Kager, B. Nienhuis, L.P. Kadanoff. Exact solutions for Loewner evolutions. *J. Stat. Phys.* 115:805–822, 2004. arXiv: math-ph/0309006.
25. W. Kager, B. Nienhuis. A guide to stochastic Löwner evolution and its application. *J. Stat. Phys.* 115:1149–1229, 2004. arXiv: math-ph/0312056.
26. G. F. Lawler. Hausdorff dimension of cut points for Brownian motion. *Electron. J. Probab.* 1:1–20, 1996.
27. G. F. Lawler. The dimension of the frontier of planar Brownian motion. *Elect. Comm. Probab.* 1:29–47, 1996.
28. G. F. Lawler. Geometric and fractal properties of Brownian motion and random walk paths in two and three dimensions. In *Random Walks (Budapest, 1998), Bolyai Society Mathematical Studies*, volume 9, pages 219–258, 1999.

29. G. F. Lawler. An introduction to the Stochastic Loewner Evolution. Available online at URL http://www.math.duke.edu/%7Ejose/esi.html, 2001.
30. G. F. Lawler and W. Werner. Intersection exponents for planar Brownian motion. *Ann. Prob.* 27(4):1601–1642, 1999.
31. G. F. Lawler, O. Schramm, and W. Werner. Values of Brownian intersection exponents I: Half-plane exponents. *Acta Math.* 187(2):237–273, 2001. arXiv: math.PR/9911084.
32. G. F. Lawler, O. Schramm, and W. Werner. Values of Brownian intersection exponents II: Plane exponents. *Acta Math.* 187(2):275–308, 2001. arXiv: math.PR/0003156.
33. G. F. Lawler, O. Schramm, and W. Werner. Values of Brownian intersection exponents III: Two-sided exponents. *Ann. Inst. H. Poincaré Statist.* 38(1):109–123, 2002. arXiv: math.PR/0005294.
34. G. F. Lawler, O. Schramm, and W. Werner. Analyticity of intersection exponents for planar Brownian motion. *Acta Math.* 189:179–201, 2002. arXiv: math.PR/0005295.
35. G. F. Lawler, O. Schramm, and W. Werner. One-arm exponent for critical 2D percolation. *Electron. J. Probab.* 7(2):13 pages, 2001. arXiv: math.PR/0108211.
36. G. F. Lawler, O. Schramm, and W. Werner. Conformal invariance of planar loop-erased random walks and uniform spanning trees. *Ann. Prob.* 32:939–995, 2001. arXiv: math.PR/0112234.
37. G. F. Lawler, O. Schramm, and W. Werner. On the scaling limit of planar self-avoiding walk. In *Fractal geometry and application, A jubilee of Benoît Mandelbrot*, *Amer. Math. Soc.* Proc. Symp. Pure Math. 72, Amer. Math. Soc., Providence RI, 2004. arXiv: math.PR/0204277.
38. G. F. Lawler, O. Schramm, and W. Werner. Conformal restriction: the chordal case. *J. Amer. Math. Soc.* 16(4):917–955, 2003. arXiv: math.PR/0209343.
39. K. Löwner. Untersuchungen über schlichte konforme Abbildungen des Einheitskreises. I. *Math. Ann.* 89:103–121, 1923.
40. B. Nienhuis, A.N. Berker, E.K. Riedel and M. Schick. First- and second-order phase transitions in Potts models; a renormalization-group solution. *Phys. Rev. Lett.* 43:737 1979.
41. B. Nienhuis. Exact critical point and exponents of the O(n) model in two dimensions. *Phys. Rev. Lett.* 49:1062–1065, 1982.
42. B. Nienhuis. Critical behavior of two-dimensional spin models and charge asymmetry in the Coulomb Gas. *Journal of Statistical Physics* 34:731–761, 1984. Coulomb Gas formulation of two-dimensional phase transitions. In C. Domb and J. L. Lebowitz, editors, *Phase transitions and critical phenomena*, volume 11, pages 1–53. Academic Press, London, 1987.
43. B. Nienhuis. Locus of the tricritical transition in a two-dimensional q-state Potts model. *Physica A* 177:109–113, 1991.
44. S. Rohde and O. Schramm. Basic properties of SLE. *Ann. Math.* 161:879–920, 2005. arXiv: math.PR/0106036.
45. H. Saleur and B. Duplantier. Exact determination of the percolation hull exponent in two dimentions. *Phys. Rev. Lett.* 58:2325–2328, 1987.
46. O. Schramm. Scaling limits of loop-erased random walks and uniform spanning trees. *Israel J. Math.* 118:221–288, 2000. arXiv: math.PR/9904022.
47. O. Schramm. A percolation formula. *Elect. Comm. Probab.* 6:115–120, 2001. arXiv: math.PR/0107096.
48. O. Schramm and S. Sheffield. The harmonic explorer and its convergence to SLE_4. *Ann. Prob.* 33:2127–2148, 2003. arXiv: math.PR/0310210.
49. O. Schramm, S. Sheffield, D. B. Wilson. Conformal radii for conformal loop ensembles. arXiv:math/0611687.
50. S. Sheffield. Exploration trees and conformal loop ensembles. arXiv:math/0609167.
51. S. Smirnov. Critical percolation in the plane: conformal invariance, Cardy's formula, scaling limits. *C. R. Acad. Sci. Paris Sér. I Math.* 333(3):239–244, 2001. A longer version is available at URL http://www.math.kth.se/∼stas/papers/.
52. S. Smirnov and W. Werner. Critical exponents for two-dimensional percolation. *Math. Res. Lett.* 8:729–744, 2001. arXiv: math.PR/0109120.
53. S. Smirnov. Conformal Invariance in random cluster models. I Holomorphic fermions in the Ising model, 2007. arXiv:0708.0039.

54. W. Werner. Random planar curves and Schramm-Löwner Evolutions. *Lecture notes from the 2002 Saint-Flour summer school* Springer, 2003. arXiv: math.PR/0303354.
55. W. Werner. Conformal restriction and related questions. 2003. arXiv: math.PR/0307353.
56. W. Werner, Girsanov's transformation for $\mathrm{SLE}_{\kappa,\rho}$ processes, intersection exponents and hiding exponents. 2003. arXiv:math/0302115.
57. W. Werner. The conformally invariant measure on self-avoiding loops. *J. Amer. Math. Soc.* 21:137–169, 2005. arXiv:math/0511605.
58. W. Werner. Some recent aspects of random conformally invariant systems. arXiv:math/0511268.
59. W. Werner. SLEs as boundaries of clusters of Brownian loops. *C. R. Acad. Sci. Paris* to appear. arXiv:math/0308164
60. D. B. Wilson. Generating random spanning trees more quickly than the cover time. In *Proceedings of the Twenty-eighth Annual ACM Symposium on the Theory of Computing (Philadelphia, PA, 1996)*, pages 296–303, New York, 1996. ACM.
61. F.Y. Wu. The Potts model. *Rev. Mod. Phys.* 54:235, 1982.